EJMSE

A NEW PREDICTIVE EQUATION FOR PUNCHING SHEAR STRENGTH OF REINFORCED CONCRETE FLAT SLABS BASED ON NUMERICAL PARAMETRIC STUDY

Berhanemeskel BIYAN[1*], Akanshu SHARMA[2,3], Esayas FTWI[1], Josko OZBOLT[3]

[1]Addis Ababa Institute of Technology, School of Civil and Environmental Engineering,
Addis Ababa university, King George IV 385, Ethiopia.
[2]Lyles School of Civil Engineering, Purdue University, 550 Stadium Mall Drive, West Lafayette, IN 47907-2051, USA.
[3]Institute of Construction Materials Fastening and Strengthening Methods,
University of Stuttgart, Pfaffenwaldring 4 70569 Stuttgart, Germany

Abstract

The paper proposes a new equation for the prediction of punching shear strength of reinforced concrete flat slabs. The basis of the new predictive equation is a detailed numerical parametric study conducted using the nonlinear 3D finite element analysis using FE software MASA. For this, results of the previously tested flat slabs from literature are used as reference for validation of the numerical model. The numerical modelling procedure is validated with two previously tested slabs, one failing in pure punching prior to yielding of flexural rebar, and the second failing in flexure-punching which resulted in yielding followed by punching. The result shows that the load-displacement behavior, failure modes and the crack pattern are captured well by the analysis. Following the validation, a detailed parametric study is performed to investigate the influence of slab depth, concrete strength, longitudinal reinforcement ratio, column size and effect of reinforcement spacing. From the evaluation of results, it is observed that the punching resistance increases with slab depth but at a decreasing rate (size effect). The punching shear strength also increases with increasing longitudinal reinforcement ratio, concrete strength as well as the column area. All the reinforcing bars placed within a distance of 3.5 times the effective depth of the slab from the column center contributes significantly towards dowel action. With increasing column size, the deformation at the peak load also increases. Based on the evaluation of the results of the analyses, an empirical equation for the prediction of punching shear is derived. The results of the equation are compared with the results of a large experimental database of 235 tests, and it is shown that the proposed equation leads to better agreement with the test results compared to the equations given in the current codes (ACI, Canadian, Eurocode, Japanese code). The comparison shows that generally the predictions by existing equations in the codes tend to be unconservative for large slab with low reinforcement ratio.

Keywords: *punching shear; failure mode; reinforcement ratio; flexural punching; crack pattern dowel action; predictive equation.*

Introduction

In reinforced concrete structures, shear failure due to its inherently brittle nature must be avoided. In case of flat slabs, the two-way shear failure called punching shear is one such failure mode that must be prevented by design. Punching shear is identified by a cone shaped perforation due to concentrated load on slabs and or footings that start from the tension surface with a certain inclination angle θ [1].

In reinforced concrete elements the major shear resistance mechanisms in the absence of transverse reinforcement are known to be the dowel action by the longitudinal reinforcement, crack

*Corresponding author: berhane.meskel@aait.edu.et

friction or aggregate interlock, and shear stresses on un-cracked concrete in compressive zone [2]. These mechanisms are dependent on different parameters like concrete strength, flexural reinforcement ratio, slab depth and column size. Number of research have been done so far to investigate the influence of these factors on punching shear resistance of concrete slabs. Effect of concrete grade on shear resistance was first addressed by Graf (1933). He concludes that the punching resistance increases with increase in concrete strength, but the increase is not in direct relation [3].

By testing 43 new samples and using previously tested specimens, Moe (1961) relates the punching shear resistance with compressive strength of concrete through square root relation [4]. Later, it is observed that relating the punching resistance to square root of concrete compressive strength overestimates the shear capacity for high strength concrete therefore relating it to the cube root of compressive strength is more realistic [5-7].

Flexural reinforcement is known to contribute to the punching shear resistance due to dowel action. Through experimental investigations of 83 specimens, Talbot (1913) concludes that the shear capacity of slab increases with increasing in reinforcement ratio [8]. Later, Elstner and Hognestad (1956) showed that the shear strength cannot be increased by the amount of flexural reinforcement ratio which is contrary to current findings [9]. Other researchers concluded that the increase in flexural reinforcement ratio increases the punching shear resistance, but the increase is not linear [10-14].

The depth of the slab enhances punching shear capacity with a decreasing rate. This is due to size effect which results in reduction of nominal shear stress with increasing member size. This has been explained due to reduced aggregate interlock [15]. According to Bažant (1984) this happens due to fast shear crack propagation as a result of high energy release to crack the large member [16] [17]. The increasing column size (punching area) also results in increasing capacity but with nonlinear relation [18].

Given the extensive past research works, currently there exists a large database of experiment on punching shear of RC slabs. At the same time, the analytical power of existing 3D FE tools (e.g., MASA) has significantly improved through continuous developments. It is thus of high importance to revisit and assess the reliability of existing code prediction provisions for punching shear resistance of RC slabs, over a wide range of parameters and their practical variability. In this paper, a systematic numerical parametric study is performed to investigate the influence of concrete grade, flexural reinforcement ratio, slab depth and column size on punching shear strength of reinforced concrete flat slabs. Based on the evaluation of the numerical results, an empirical equation is proposed to estimate the punching shear strength of flat slabs. The results of the proposed predictive equation as well as the equations given in the existing norms are compared against the results of a large test database. It is found that the proposed equation results in better prediction of the punching shear capacity of flat slabs compared to existing code predictions.

Predictive Equations for Punching Shear Strength According to Major Building Codes

The punching shear strength predictive equation of different building codes are summarized on the table below.

Methodology

The basic methodology consists of a numerical parametric study performed to investigate the influence different parameters on punching shear strength of slabs. For the numerical investigations a 3D nonlinear finite element software is used to simulate the punching shear response of RC slabs. This software has been used to simulate different conditions like seismic performance of bema column joint, effect of impact load on reinforced concrete structures and effect of fire on concrete [47-50]. The applicability of the analytical framework is verified through

validation of experimentally tested slab from previous research before proceeding to the parametric study. From the parametric study a simplified empirical equation is derived. The prediction of the derived equation is compared with different code provisions and conclusion is drawn out of the result.

Table 1. Punching shear predictive equations of different building codes

Design Codes	Punching Shear Provisions	Control perimeter	
ACI 318 [27]	$V_c = 1/3(b_o d\lambda\sqrt{fc'})$, MPa and mm		
CSA [28]	$V_c = 0.38(b_o d\lambda\sqrt{fc'})$, MPa and mm		
Eurocode 2 [26]	$v_{Rd,c}= (0.18k\,(100r_l f_{ck})^{1/3})b_o d$		
JSCE [29]	$Vpcd= \beta_d\beta_p\beta_r f_{pcd}U_p d$, MPa and mm	ACI, Canadian and JSCE Code	Eurocode 2
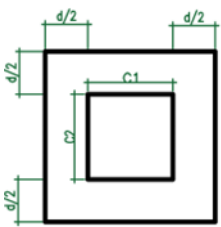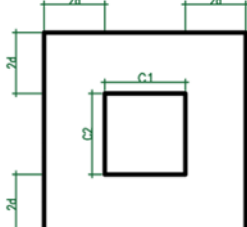
Brief Description of the 3D Nonlinear FE Framework (MASA)

For the validation and parametric study, a numerical modelling software called MASA (Macroscopic space analysis) is used which is developed in university of Stuttgart. In MASA microplane material model with relaxed kinematic constraint is employed as constitutive law. It is aimed to be used for nonlinear three-dimensional damage and fracture analysis of concrete and reinforced concrete structures in the framework of the smeared crack approach. The fundamental property of the microplane model is the interaction between various orientations, which are defined by microplanes. The microplanes may be imagined representing damage planes or weak planes in the microstructure. 3D damage and fracture analysis are carried out in the framework of the smeared crack approach. To avoid error related to mesh size the constitutive law is coupled with the localization limiter of local integral type (crack band method). In this method the energy dissipation due to crack formation is equalized with the concrete fracture energy. For more detail about the FE tool one can refer [21].

Concrete is modeled as a solid element with four nodes tetrahedral element as shown in Fig. 1. The stress strain diagram of both tension and compression is also defined. The steel reinforcement bar is modeled using solid eight node hexahedral elements. Depending on the discretization of reinforcement, 1D truss or 3D solid finite elements, uniaxial elasto-plastic stress-strain relationship with or without strain hardening or classical plasticity-based models can be employed. The bond model used in the code is based on the discrete bond-slip relationship that is defined by zero length non-linear spring elements [21]. In our case It is assumed that there is a perfect nodal connectivity between concrete and steel.

a)   b)
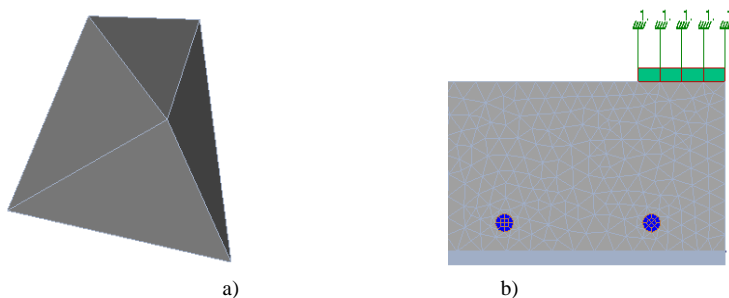
Fig. 1. a) tetrahedron mesh of concrete; b) modeling of steel, concrete and loading plate
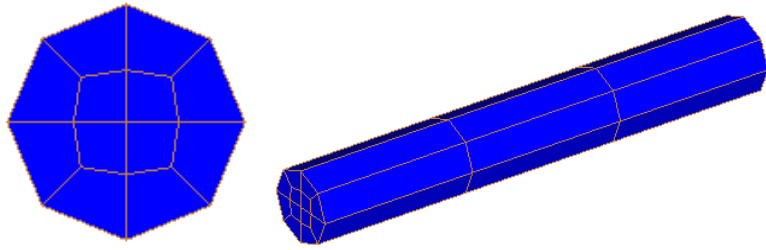
Fig. 2. Hexahedron mesh of steel

Validation of Numerical modeling

To study the punching shear behavior of flat slabs with low flexural reinforcement Muttoni Guandalini, et al. [19] performed 11 experiments with varying flexural reinforcement ratio and member size. From these experiments test PG6 is used for validation here. This test specimen is selected because it is adequately reinforced in flexure as a result punching shear failure can be observed clearly. Furthermore, specimen PM2 tested by Fernández et al [20] was selected for validation. The specimen is selected because it is lightly reinforced in flexure and flexural reinforcements yield prior to punching shear failure. They tested 20 slabs (photographic view of PM2 is shown on Fig. 3 c) to study the effect of integrity reinforcement on progressive failure of slab due to punching shear [20]. The detailed geometry and material property of slabs PG6 and PM2 are summarized on Table 2.

Table 2. Geometry and Material Property of slabs validated

Parameter	Units	PM2	PG6	Parameter	Units	PM2	PG6
Slab Width, B	mm	1500	1500	Yield Strength of Steel, f_y	MPa	601	526
Slab Length, L	mm	1500	1500	Ultimate Strength of Steel, f_u	MPa	664	607
Slab Depth, h	mm	125	125	Modules of Strain Hardening, E_{sh}	MPa	3000	3000
Slab Cover, d'	mm	23	29	Flexural Reinforcement Ratio, ρ	%	0.49	1.5
Column Size, c	mm	130	130	Modules of Elasticity of Concrete, E_c	GPa	29	28
Slab Effective Depth, d	mm	102	96	Compressive Cylindrical Strength, $f_c^{'}$	MPa	36.5	34.7
Flexural Rebar Area, A_s	mm²/m	500	1440	Concrete Tensile Strength, $f_{ct}^{'}$	MPa	3.3	3.23

The flat slabs from the two experiments are different in terms of their failure mode. Specimen PG6 fails in pure punching where the concrete fails prior to yielding of flexural reinforcement. Specimen PM2 fails in flexure-punching where punching shear occurs after the flexural reinforcements have yielded.

As the slabs are symmetric about two orthogonal planes, only a quarter model of the slab is used in the analysis for optimizing the run-time of the simulations. This might increase the estimated load capacity. The symmetry is a broken symmetry after the onset of crack.

The crack patterns (failure modes) obtained for specimen PG6 is shown in Fig. 4, while the load-displacement curves are plotted in Fig. 5. The results of the numerical analysis for specimen PG6 are in good agreement with the experimental result. In the experiment it was reported that the failure mode was pure punching. Most of the flexural reinforcement were stressed below the elastic limit. The numerical model also fails in pure punching prior to yielding of flexural reinforcements. The peak load at failure and the corresponding deflection at failure are consistently captured. The load-displacement diagram obtained from the analysis follows the same path as the experimental result (Fig. 5). The peak load and deformation are estimated with a nominal difference from the test results of 1.68% and 6.78%, respectively.
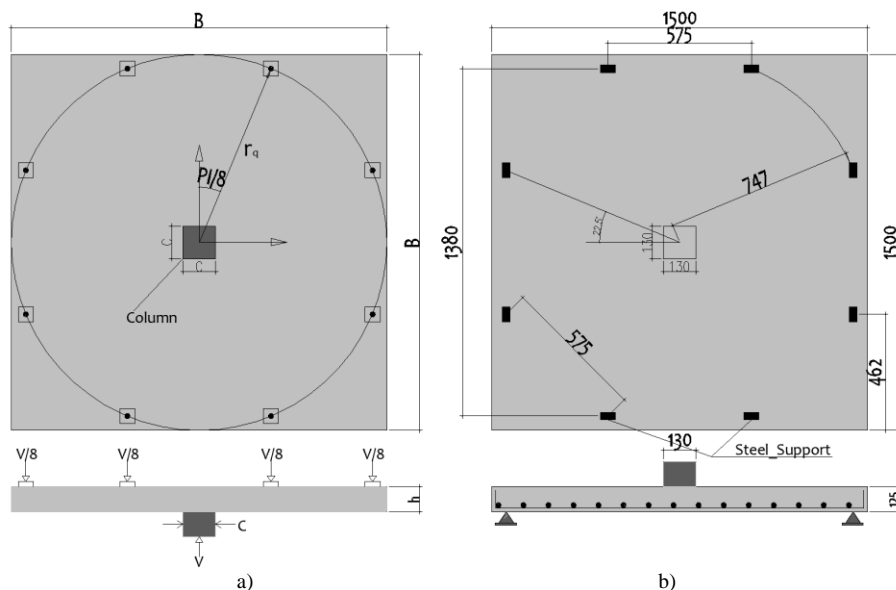
Fig. 3. Schematic drawing of slabs used for numerical validation:
a) PG6 [19] b) PM2 [20], c) experimental setup of PM2 [20]

At first, flexural cracks appear under the loading points (location of maximum bending moments) as shown in Fig. 4 a this is also shown at point 'a' of the load deformation diagram Fig. 5. The peak load corresponds to the formation of the major shear crack this is point 'b' of the load deformation diagram Fig. 5. Until this point there is an increase in shear capacity as the shear transfer is still there even after crack. At peak load (point 'b' of Fig. 5) around 87% of the steel strength is utilized. This flexural reinforcement is located at the mid span of the slab where maximum moment is expected to occur. Hence, the failure mode corresponds to pure punching shear failure, without yielding of reinforcement as reported in the experiment [19].
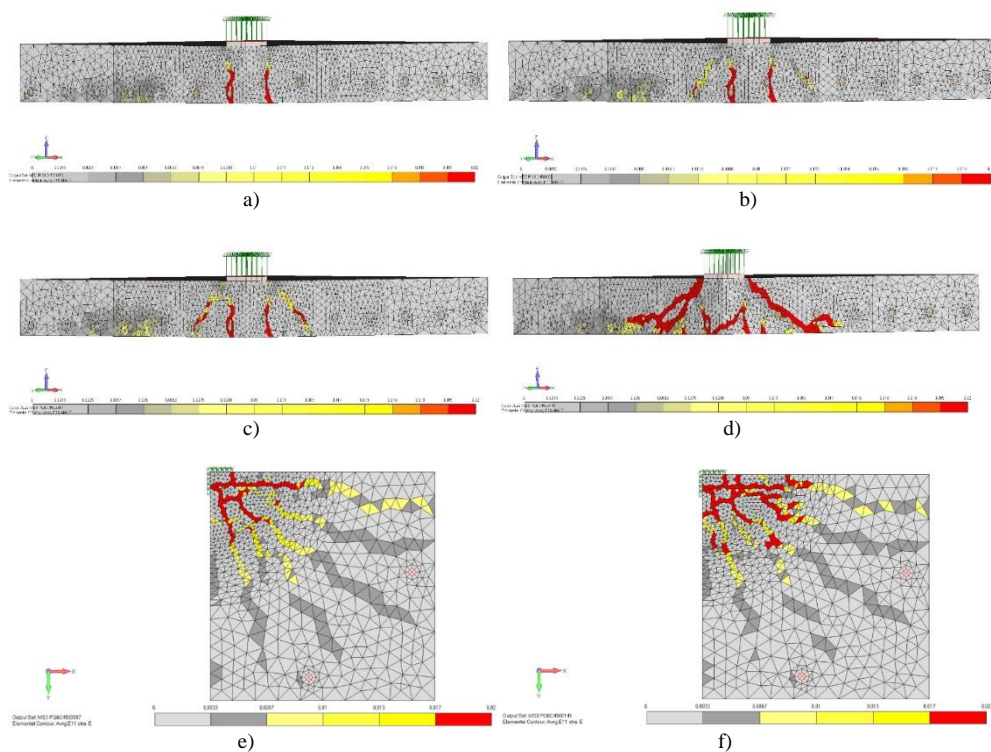
Fig. 4. Specimen PG6 crack propagation: a) flexural crack; b) onset of shear crack; c) crack at peak load;
d) Post punching crack; e) plan view of flexural crack at peak load;
f) plan view of flexural crack after punching failure at ultimate load

The results obtained by the numerical analysis of specimen PM2 [20] are also in good agreement with the experimental results. The load-displacement curves displayed in **Fig. 5** show a good overall correspondence between experimental and numerical results. The peak load prediction capacity is acceptable and demonstrates a variation of 0.21% from the experiment. However, there is a visible difference in the initial stiffens between the experimental and analytical results. This is caused) due to the drying shrinkage induced self-equilibrated stresses in the slab prior to loading, which influences the initial stiffness of the experimental specimen [46]. This drying shrinkage effect was not introduced in the numerical modeling as there is no information reported on the experimental data about the drying shrinkage. The post peak response shows a rapid degradation due to fracture of concrete followed by rupture of the flexural reinforcement which was also reported in the experiment this is related to point 'e' of Fig. 5.

The predicted failure mode is flexural failure followed by punching shear, which can be seen from the crack propagation shown in Fig. 6. As the load increases the flexural cracks are intercepted by the shear crack around the mid-section of the slab. Before reaching the peak load, the flexural rebar yields which results in relatively large displacement of the slab before peak. Fig. 6 (a) shows flexure and shear crack at yielding of the rebar in (b) the crack becomes larger and deeper as the rebar has yielded which leads to (c) where the rebar reaches its ultimate stress capacity. Even after the peak load the strain of the steel is $3.3\%_o$ this indicates the rebar has not fractured. This observation asserts that the final mode of failures governed by crushing of concrete.
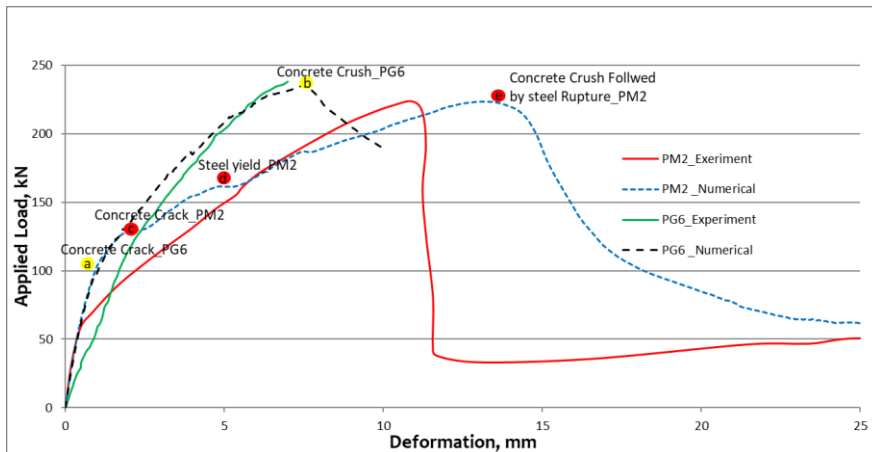
Fig. 5. Load deformation diagram of experimental and numerical modeling of PG6 & PM2
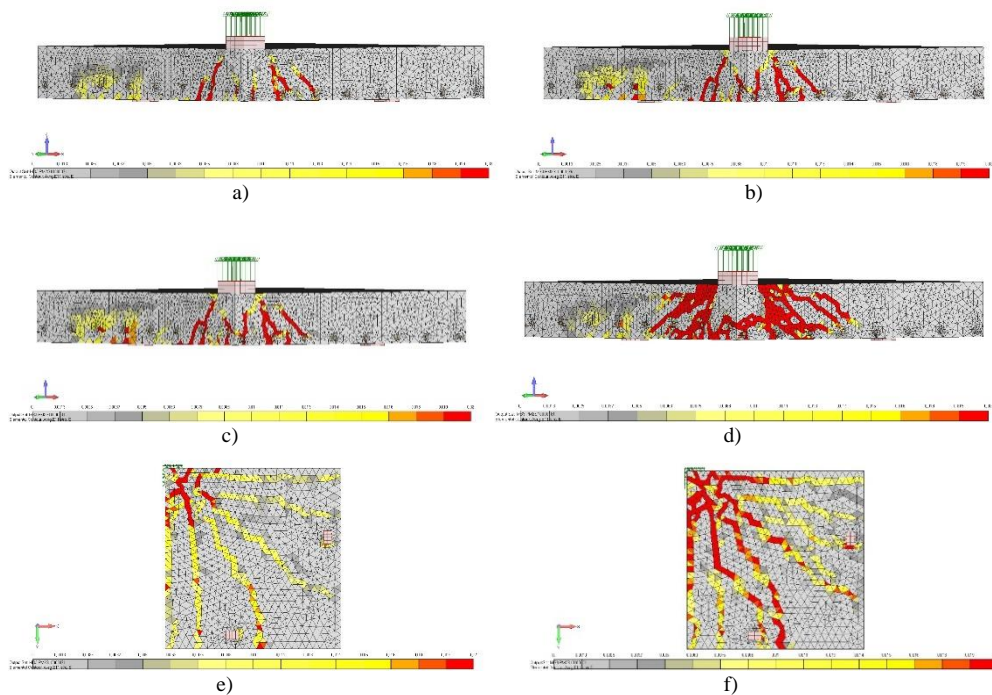
Fig. 6. Specimen PM2 crack propagation: a) flexure-shear crack at yielding; b) onset of ultimate Rebar stress;
c) crack at peak load (ultimate rebar stress); d) post peak crack pattern;
e) plan view of flexural crack at rebar yielding; f) plan view of flexural crack at ultimate rebar stress

In PM2, the width of the flexural crack increases which is expected for slab with lower amount of flexural reinforcement. The failure mode reported in Fig. 6 corresponds well with the results reported in [20].

Parametric study

After validations, the numerical simulation was used to carry out a detailed parametric study in which the influence of major parameters on punching shear strength were evaluated. At

a time, only one parameter was varied while keeping all other parameters constant. The chosen parameters are concrete strength [C-Series], slab thickness [D-Series], steel reinforcement ratio [ρ -Series], and column size [P-Series]. Table 3 summarizes the different combination of parameters used in this study. A total of 28 cases are considered. In all cases diameter 20mm with a spacing of 100mm are used as flexural reinforcement and slab dimensions are kept as 1500x1500mm. For the C-series two sets of groups were used, (i) with low flexural reinforcement (ρ=0.49% diameter 8mm bar at every 100mm) and (ii) with high flexural reinforcement (ρ=1.5% diameter 20mm bar at every 100mm).

Table 3. Slab Naming and Varied Parameters

Series	Model Name	Mean Strength (MPa)	Flexural Rebar Ratio ρ (%)	Slab Depth d (mm)	Square Loading Plate (mm)
C-Series	PMρC25	28			130x130
	PMρC35	36			
	PMρC45	44			
	PMρC55	52			
	PMρC65	60	1.5 & 0.49	125	
	PMρC75	68			
	PMρC85	76			
	PMρC100	88			
	PMρC120	104			
ρ-Series	PMρρ0.49		0.49		
	PMρρ0.80		0.80		
	PMρρ1.0	36	1.00	125	130x130
	PMρρ1.5		1.50		
	PMρρ2.0		2.00		
D-Series	PMρD100			63.95	130x130
	PMρD125			87.10	
	PMρD200			157.65	
	PMρD225			181.39	
	PMρD250	36	1.50	205.2	
	PMρD300			253.02	
	PMρD400			349.18	
	PMρD500			445.82	
	PM2D500			463.10	
P-Series	PMρP10				100x100
	PMρP13				130x130
	PMρP16	36	1.50	125	160x160
	PMρP20				200x200
	PMρP25				250x250
	PMρP30				300x300

Results and Discussion

Effect of Slab Depth (D-Series)

The slab total depth is varied from 100mm to 500mm with a constant reinforcement ratio and spacing. This resulted in an effective depth varied from 63.95 mm to 445.8 mm. As expected, increasing slab depth leads to an increase of punching shear resistance of the slab. The failure load obtained from the numerical analysis is plotted as a function of the slab total depth in Fig. 7. The overall trend of increasing punching shear failure load of the slab with increasing effective depth of the slab lies within the trends of different predictive equations. In addition to increase in the load carrying capacity, increasing the slab depth changes the load-deflection diagram from relatively flat to sharper peak which is accompanied by smaller deformation at failure. The slab with 100mm total depth (PMρD100) reaches peak at a relatively large deformation and as the

depth increase peak load deformation decreases. As the slab depth increases the post peak load-deflection diagram becomes steeper.

As shown in Fig. 8 PMρD500 and PM**2**D500 differ only in the amount of flexural reinforcement ratio where it is reduced from 1.5% to 0.49%. This change results in 15% shear capacity reduction which shows the influence of reinforcement ratio on punching shear capacity. This strength reduction is also shown on Fig. 7 with a 'Square ' on the right extreme side. As the slab depth increase from PMρD100 to PMρD500 the cracking load also seem to increase with it. This phenomenon was explained by Li [25]. As the slab depth increases the failure mode changes from flexural failure to flexure punching and finally to punching shear failure.
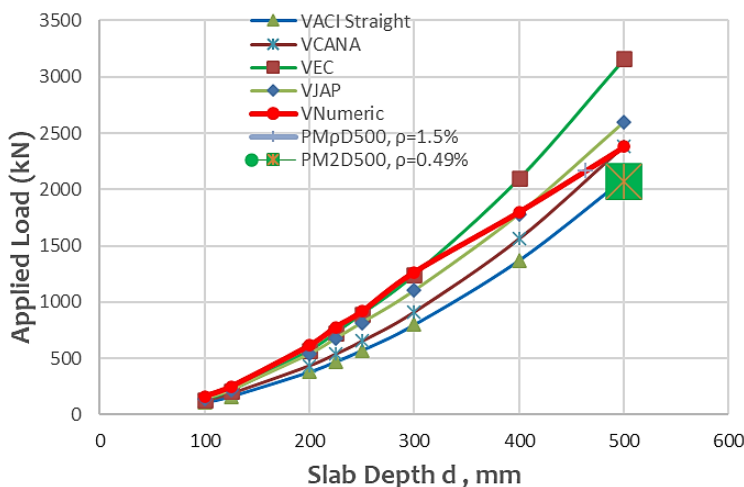
Fig. 7. Effect of Slab depth on punching shear capacity
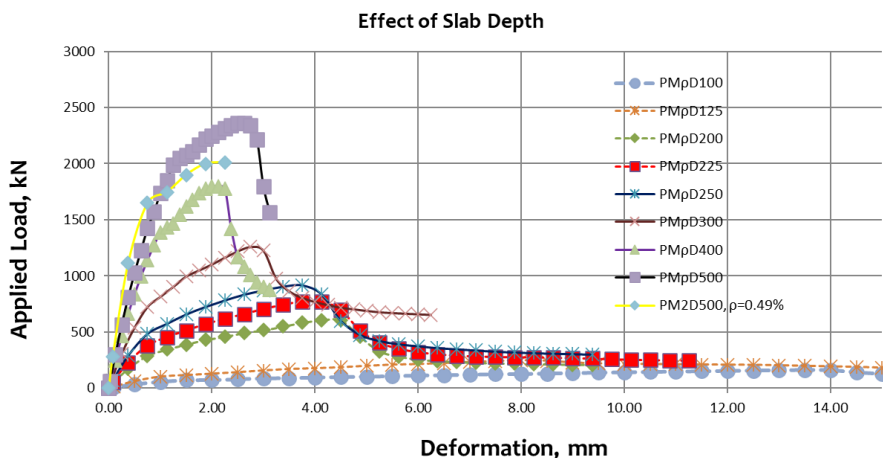
Fig. 8. Effect of slab depth on load deformation diagram

The failure shear stress is shown to reduce as the slab depth increases. This is explained as size effect by different researchers [16][17][25]. The punching shear failure load increases roughly as a function of $d^{1.5}$, which is due to the attributed to the size effect of concrete. The punching shear area is proportional to d^2, while the consideration of highest size effect would result in the punching shear strength inversely proportional to $d^{0.5}$, thus resulting in an overall

dependency of the punching shear failure load to $d^{1.5}$. This is analogous to the concrete cone breakout failure load in case of anchorages [51] (Eligehausen et al., 2006). Fig. 9 shows the relation between slab depth and failure shear stress. The slab depth increment also results in reduced percentage utilization of flexural reinforcement. As the slab depth vary from 100mm to 500mm the flexural rebar utilization reduces from 86% to 58.6%. This reduction is shown on Fig. 9 where higher percentage reduction is seen when the slab depth changes from 150mm to 200mm.

a)

b)
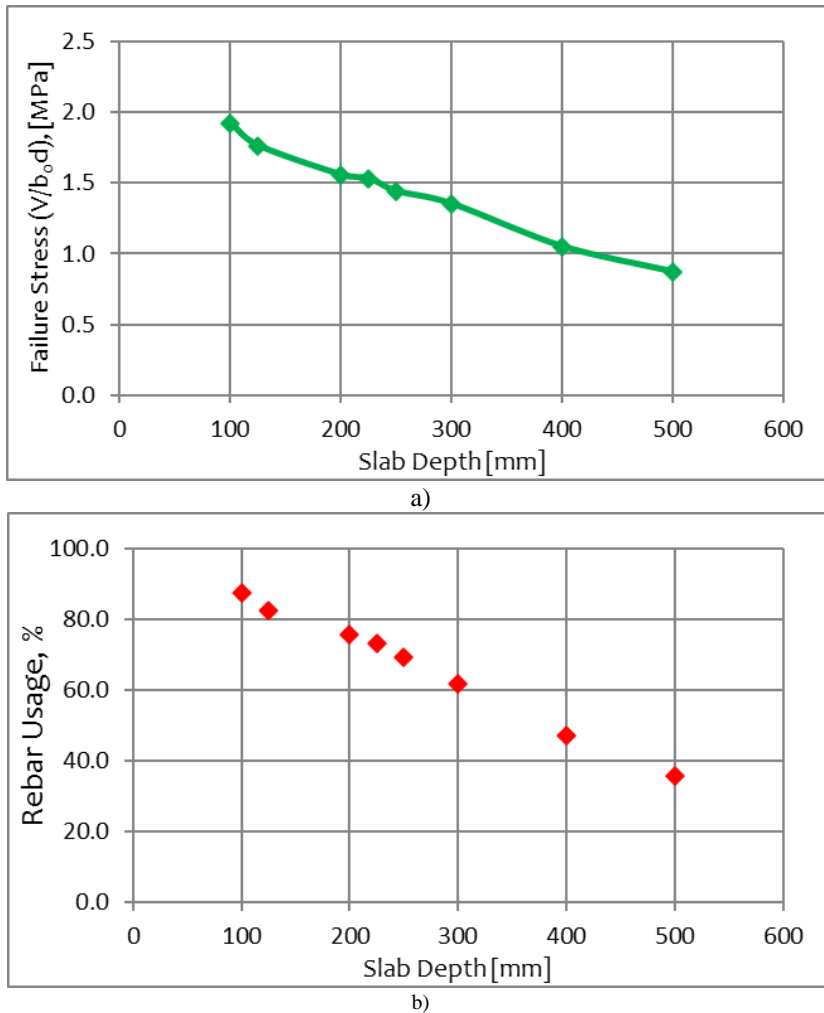
Fig. 9. Effect of slab depth on: a) failure stress b) percentage reinforcement utilization

The inclined shear crack becomes more dominant when the depth of the slab increases, which is evidenced in Fig. 10. Fig. 10 a) shows crack pattern of PMρD100 where the flexural cracks are predominant whereas on Fig. 10 g) less flexural cracks with concentrated inclined shear cracks is observed.
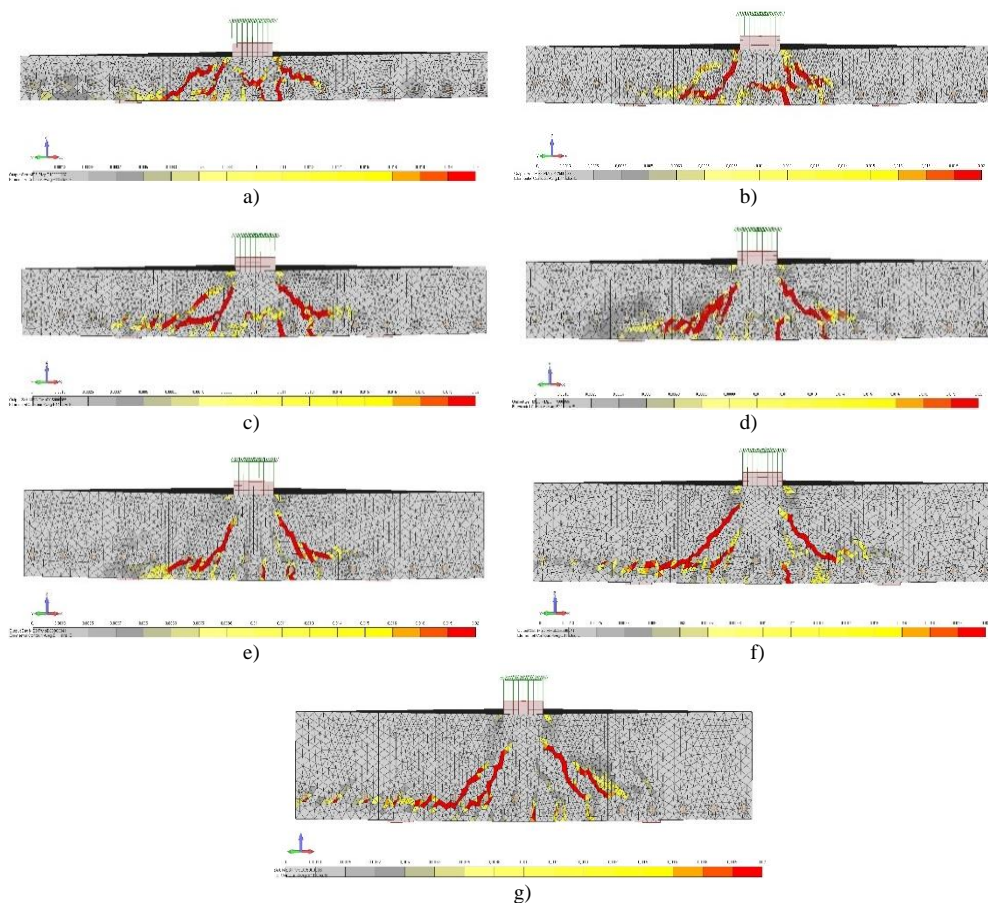
Fig. 10. Progress of crack pattern with depth for: a) 100mm slab depth, b) 125mm slab depth, c) 200mm slab depth d) 225mm slab depth, e) 300mm slab depth, f) 400mm slab depth and g) 500mm slab depth

Effect of concrete grade (C-Series)

Generally, it is observed that increasing concrete strength increases the punching shear force. For slabs with adequate flexural reinforcements, [PMρ C_series], increasing the concrete grade results in higher punching shear capacity. This continues until the failure mode changes to flexural punching where steel yielding happens before punching. The capacity increment rate reduces when the concrete grade reaches 75MPa. Increasing the concrete grade beyond this value has shown reduced peak load increment. In Fig. 11 it is shown that the increment rate becomes flatter after 75MPa. This is due to the change in failure mode. As increasing the concrete grade from low to high strength the brittle punching failure mode changes to flexure-punching failure. This is due to higher flexural rebar utilization with higher concrete grade, which finally results in yielding of more flexural reinforcements.

For lightly reinforced slabs [PM2 C_series] the punching shear capacity increase with concrete grade until 45MPa. After that the capacity keeps increasing but with reduced slope. The reduction in increment is due to change in failure mode where it changes to flexural yielding. Effect of concrete grade on load-deflection diagram for both series is shown in Fig. 11.

As the concrete strength becomes higher the descending branch of the load deformation diagram becomes steep. Hence the high concrete strength usage results in a more brittle post peak load deformation diagram. This is believed to be due to smooth crack formation in high strength concrete which results in loss of interface shear transfer mechanism.
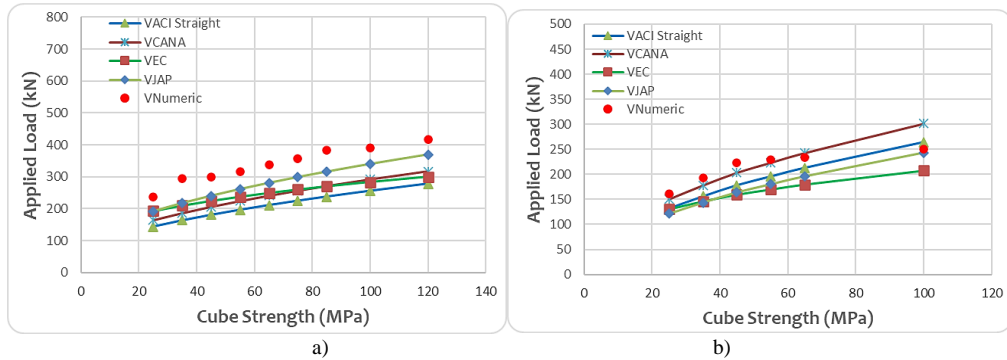
Fig. 11. The effect of concrete grade on punching strength:
a) adequately reinforced slab (ρ=1,5); b) lightly reinforced slab (ρ=0, 49)

a)

b)
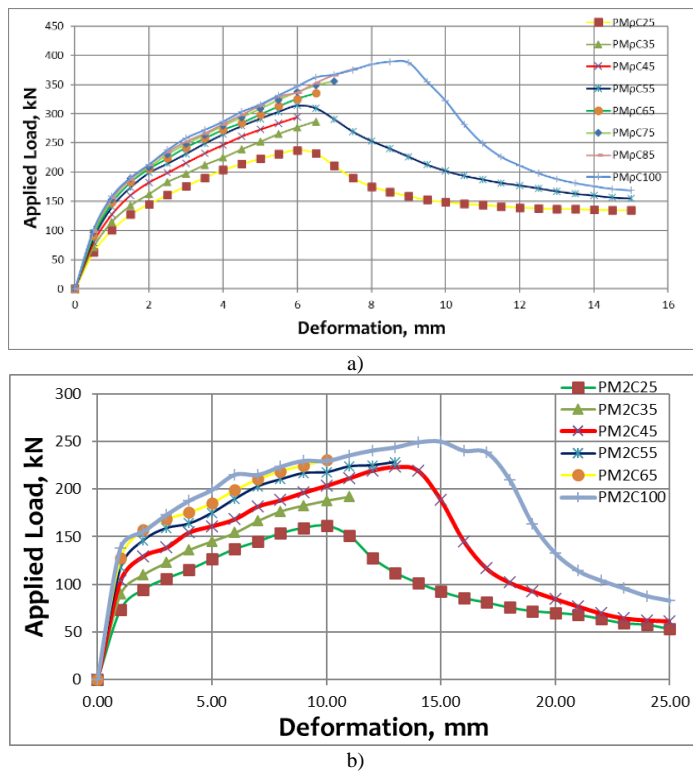
Fig. 12. The effect of concrete grade on Load deformation diagram:
a) adequately reinforced slab (ρ=1,5); b) lightly reinforced slab (ρ=0, 49)

As the concrete grade increases the materials are utilized to their full capacity. This results in higher load carrying capacity and more cracks are visible this can be seen from Fig. 13. The result shows that crack pattern is not perfectly symmetrical. This is because of the analysis sequence. The numerical analysis starts from elements and nodes on one end and continue to elements on the other ends. This will result in different stiffness on opposite side of the loading column, hence leading to broken symmetry.
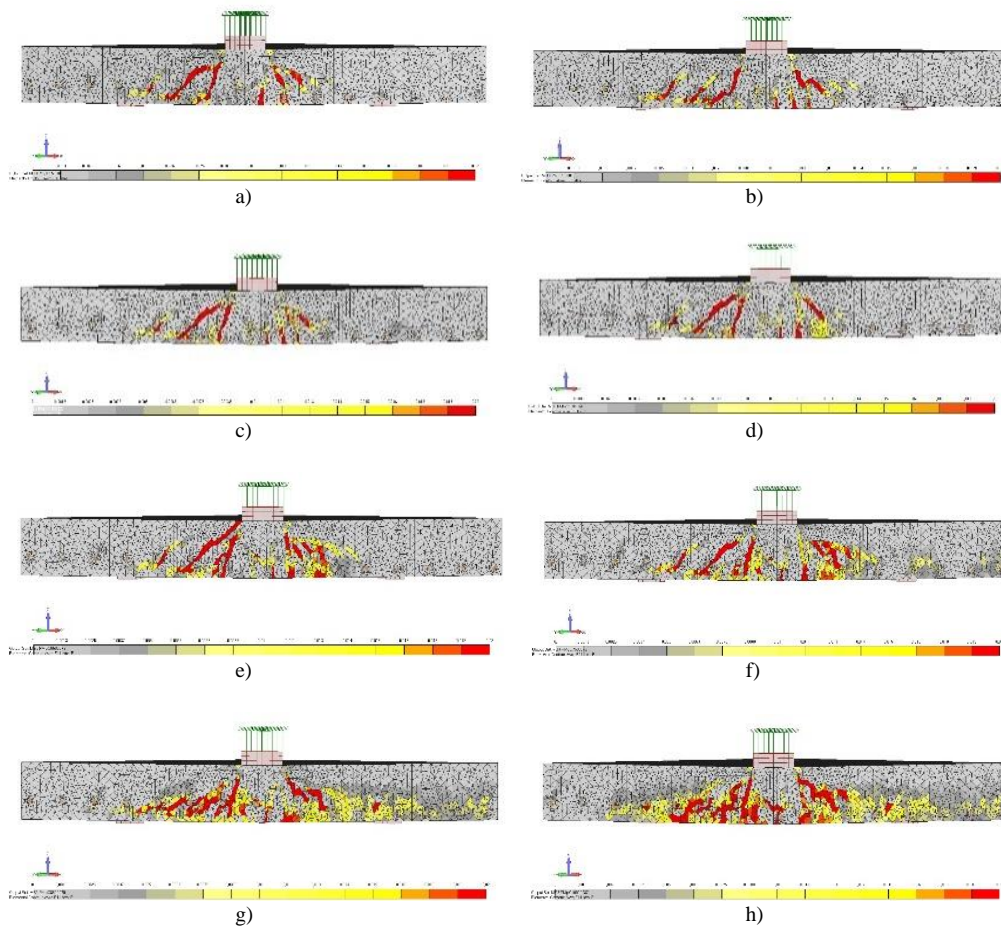
Fig. 13. Crack pattern at failure load for concrete grade of a) C-25 b) C-35 c) C-45 d) C-55 e) C-65 f) C-75 g) C-85 h) C-100

The gradual reduction of capacity increment rate mentioned earlier can be related to the increase in percentage utilization of flexural rebar. This is because even if the concrete capacity is higher the steel cannot take additional load beyond its ultimate stress capacity.
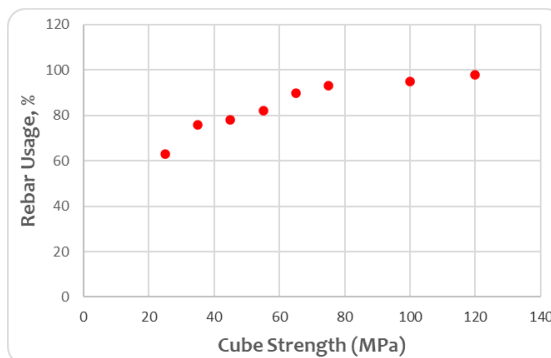
Fig. 14. Percentage utilization of flexural reinforcement

Effect of Reinforcement ratio (ρ-Series)

In the parametric study it is observed that increasing the flexural reinforcement results in higher punching shear capacity. As the flexural reinforcement ratio increases from 0.49% to 2.0% the failure mode changes first from flexure to flexure-punching and finally from flexure-punching to pure punching it also results in 33% increase in the punching shear force. In the study it is seen that only flexural reinforcements at a radius of 3.5d from column center are mobilized for dowel action. It is also seen that this reinforcement not only changes the failure mode but also enhance the punching shear capacity significantly in a relation of fourth root like the suggestion of Long [22]. It is observed that increasing the flexural reinforcement increases the punching capacity with steep slope up to certain point. Beyond this value the dowel action contribution becomes minimal. For the given geometry of slab, the increment become minimal beyond 1.5% reinforcement ratio this is evidenced on Fig. 15 and Fig. 16.

Increasing the flexural rebar has resulted in more brittle failure where the peak load deformation reduces gradually. This is grouped in three zone which is shown on Fig. 15. Zone one shows steeper deformation reduction and is seen is at lower flexural reinforcement ratio [PM$\rho\rho$0.49 - PM$\rho\rho$0.8]. The failure is flexural failure with larger peak load deformation. Zone two shows constant deformation and it is seen at moderate flexural reinforcement ratio [PM$\rho\rho$0.8 & PM$\rho\rho$1.5]. On zone three there is a gentle reduction on peak load deformation. As it is adequately reinforced [PM$\rho\rho$1.5 - 8 PM$\rho\rho$2.0] it fails in pure punching. The three zones are summarized on Fig. 15 b.

a)   b)
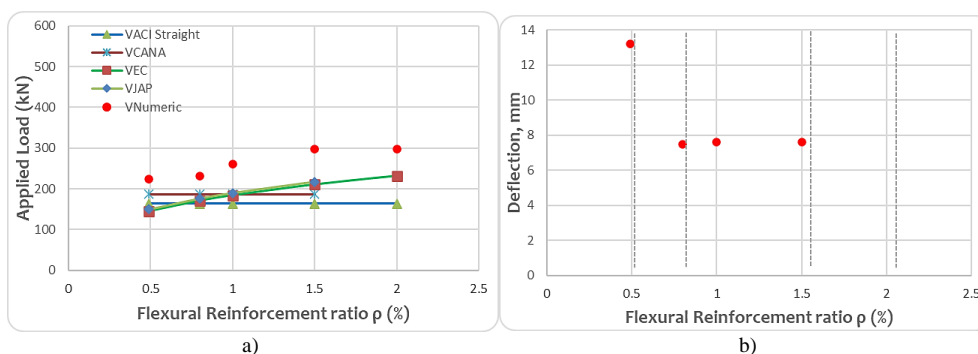
Fig. 15. The effect of dowel action on: a) failure load; b) peak load deformation (add discussion)

As it can be seen from Fig. 16 lower reinfrocment ratio results in more ductile type of failure. This is because even though the slabs finally fails in punching they will go large defromation before failure as the flexural rebar yieldes. This is clearly seen on PM$\rho\rho$0.49 where the reinforcment bar yields and reach to ultimate flexural stress. In PM$\rho\rho$0.8 yielding of flexural reinfrcment is observed. But befrore ultimate stress is reached concrete crushes which results in flexure punching type of failure.

The percentage use of the flexural rebar reduces as the amount of reinforcement ratio increases this results in a more brittle but larger failure load. Fig. 17 shows reduction of reinforcement utilization with increasing of reinforcement ratio.

It is observed that the presence of large amount of flexural reinforcement ρ like in PM$\rho\rho$1.5 and PM$\rho\rho$2.0 results in larger compression zone which reduces the tension zone and resulted in smaller bending crack. The reduced bending crack enhances the mechanism of shear transfer which is also explained by Regan [23]. The reinforcement also reduced the width of the crack which makes the interface shear transfer (aggregate interlock) more effective which also makes the dowel action higher. As the bending crack reduces the shear crack becomes more dominant and it also becomes more localized. This localization results in secondary punching

shear crack. Fig. 18 a) shows flexure dominated crack while b) to d) shows shear dominated crack at failure where the flexural crack reduces, and the shear crack becomes more pronounced.
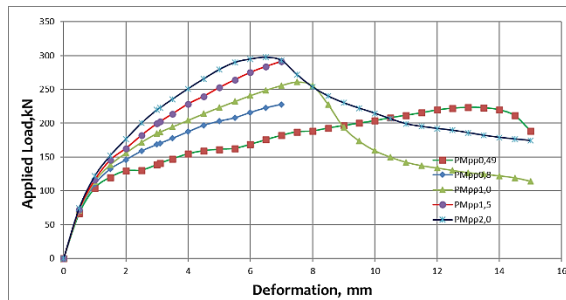
Fig. 16. The effect of flexural reinforcement on load deformation diagram
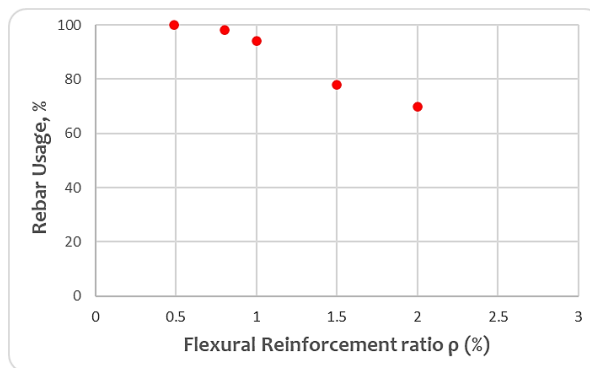
Fig. 17. The percentage reinforcement usage
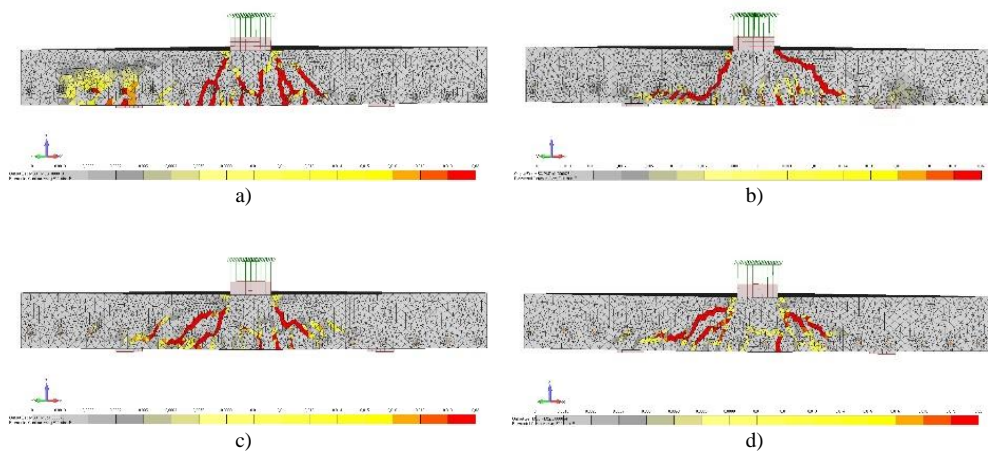
Fig. 18. Crack pattern at failure for: a) PMρρ=0.49; b) PMρρ ρ=1; c) PMρρ ρ=1.5; d) PMρρ ρ=2

As can be seen from
Fig. 19 below on the bottom surface (tension side) of the slab the crack pattern is more sever when the flexural reinforcement ratio is small as in PMρρ0.49. Increasing the flexural reinforcement ratio results in reduced flexural crack at the bottom face and the crack localized

around the column. As explained by Muttoni [24] in all the ρ-series slabs the tangential crack is concentrated around the column. This is because of radial curvature which is concentrated around the column. It creates concentric cracks which vanish as we go far from the column support and only radial crack is visible on the furthest part of the slab.
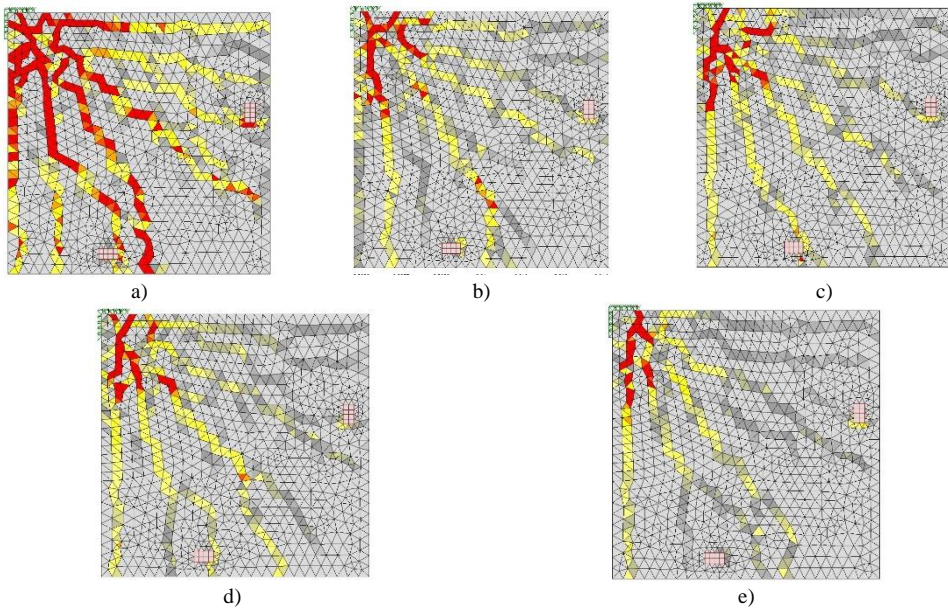
Fig. 19. Flexural crack pattern on tension side of the slab at failure (a) ρ=0.49, (b) ρ=0.8, (c) ρ=1.0, (d) ρ=1.5, (e) ρ=2.0

Effect of Column Size (C-Series)

The effect of column size is studied by changing the size of the loading plate. This is varied from 100mm to 300mm. it is observed that the changing the column size enhance the punching shear capacity. The post peak branch of the load deformation diagram also becomes more flat as the column size increase.
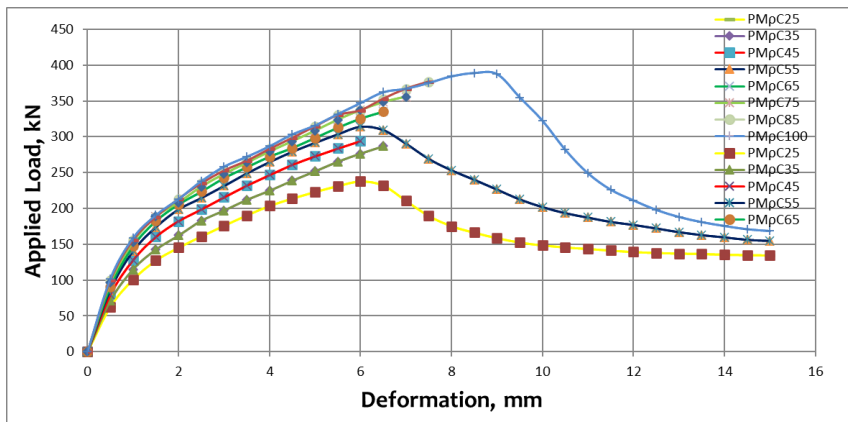
Fig. 20. Effect of column size on load deformation diagram

From Fig. 21 it is observed that the increment in punching shear strength beyond 200mm column size continues with a reduced slope.

The flexural crack at the tension side of the slab becomes more severe as the column size increases.

a)

b)   c)   d)
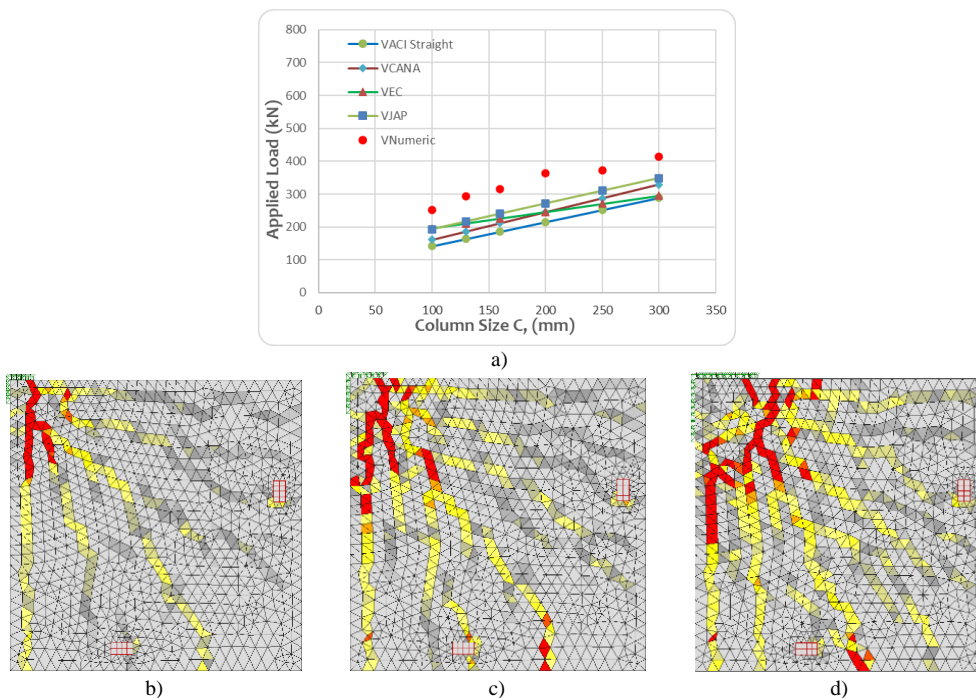
Fig. 21. The effect of column size on: a) Peak Load; c-d) crack pattern [b) C=100mm, c) C=160mm, d) C=300mm]

Effect of Reinforcement Spacing (S-Series)

The other parameter studied in this paper is the spacing of the flexural reinforcement. Its effect is seen by changing the spacing keeping the reinforcement ratio 1.5%.   a)   b)

Fig. 22 shows that effect of spacing on punching shear capacity is insignificant. It is also seen that the peak load deformation is increased slightly with increasing spacing of the reinforcement. The size of the flexural crack increase as the reinforcement spacing increase but the number of cracks reduced as the spacing increase. (Codes don not consider this spacing effect so it is in good agreement with our result).

a)   b)
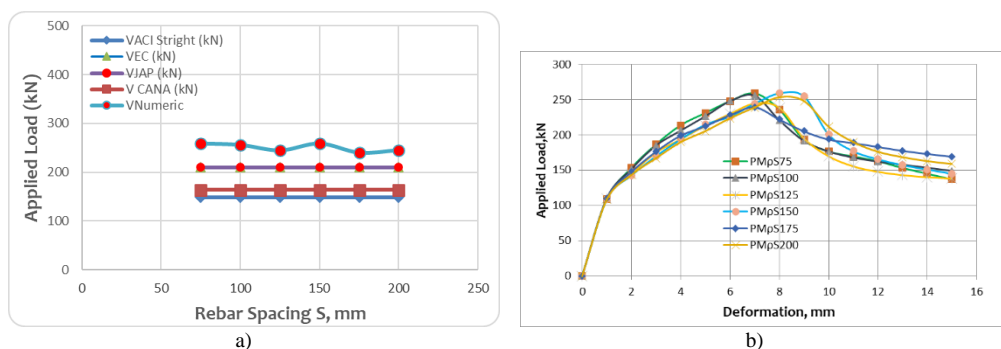
Fig. 22. The effect of Reinforcement spacing on punching shear strength:
a) Load Deformation diagram; b) effect of spacing on peak load

Comparison of Codes Prediction capacity

The result of the FE software prediction is compared with the punching shear capacity estimation of Eurocode 2 [26] Japanese code Canadian code and ACI 318-08 [27].

Generally, ACI 318-08 and Canadian code prediction is conservative for slab with normal strength concrete with conventional slab depth and high amount of flexural reinforcement. This conservativeness is more pronounced when considering rounded control perimeter. For slab with low amount of flexural reinforcement with large slab depth and high strength concrete ACI and Canadian code prediction overestimate the punching shear capacity. This is observed on PMρD500 and PM2D500 where the reinforcement changes from 1.5% to 0.49%. The punching shear capacity reduced by 15%. But this reduction is not seen on ACI and Canadian code. They both gives the same value for the two cases. this is because the two codes do not consider size effect and dowel action.

Eurocode 2 and Japanese code prediction is more accurate as they try to consider both dowel action and size effect to some extent. For large depth slab both Eurocode and Japanese code overestimate the punching shear strength. Comparing the two codes, the Japanese code's prediction results in better prediction than the Eurocode as it addresses size effect in a more realistic way. Generally, all codes give unsafe result when dealing with slab with large depth and low reinforcement ratio.

Proposed Equation

Based on the relation observed from the parametric study an empirical equation (eq. 1) is proposed.

$$V=95*(fc')^{0.4}(\rho)^{0.3}(d)^{1.45}(C)^{0.25} \tag{1}$$

The prediction accuracy is compared statistically with different codes. The result of the comparison is summarized on

Table 4. Generally, the codes prediction is conservative for most cases. All codes become unsafe when dealing with lightly reinforced high strength concrete and large member size. This can be seen from Fig. 7 and Fig. 11b. the peak load prediction for codes and proposed equation are shown on

Fig. 23.

For the derivation of the equation two sets of slab series are considered. Series one, considers slab with low amount of flexural reinforcement that fails in flexure punching and Series two is slab with adequate amount of flexural reinforcement that fails in punching shear.

After the derivation of the equation different experimentally tested slabs from previous literatures are used to see the accuracy of the prediction capacity of the proposed equation. It is observed that the proposed equation gives better prediction with coefficient of variation of 0,137 while ACI, Eurocode, Japanese code and Canadian code gives 0.231, 0.172, 0.17 and 0.231 respectively. Also, the R^2 value is 98,7% while ACI, Eurocode, Japanese code and Canadian code gives 90%, 97.2%, 98.4% and 90% respectively. This is summarized on

Table 4 below.

Table 4. Correlation of ACI Eurocode and Proposed Equation.

	ACI	EC	Japa	Cana	V_{ex}/V_{pro}
AVG	1.36	1.22	1.14	1.19	0.97
STDEV	0.315	0.209	0.195	0.276	0.151
COV	0.231	0.172	0.170	0.231	0.137
MIN	0.52	0.69	0.59	0.45	0.66
R^2	0.900	0.972	0.984	0.900	0.987

Fig. 23 shows the correlation between the experimental data from literatures with ACI, Canadian, Eurocode, Japanese code, and proposed equation prediction.
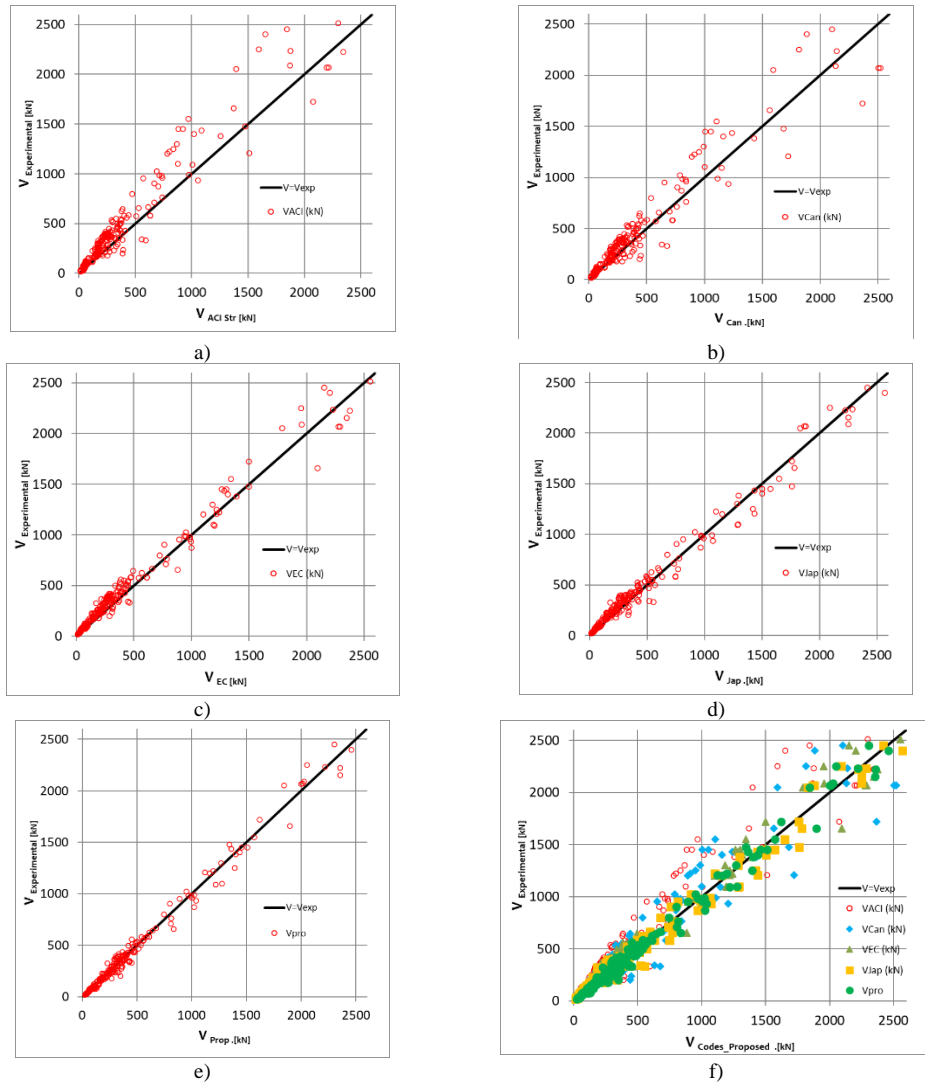
Fig. 23. Correlation of experimental value with: a) ACI; b) Canadian Code; c) Eurocode; d) Japanese Code; e) Proposed equation; f) all Codes VS Proposed equation

Conclusion

A shear critical RC slab can fail either due to flexure punching or shear punching based on the adequacy of the flexural reinforcement. Slabs adequately reinforced to avoid flexural failure fails in shear punching while slab with low amount of flexural reinforcement fails in flexure punching.

The presence of flexural reinforcement enhances the punching shear capacity by increasing the contribution of aggregate interlock and concrete strength in addition to the dowel action.

Based on the experimental data set available the ACI and the Canadian code results in conservative prediction for slab with high amount of flexural reinforcement. Their prediction result is un conservative result for slabs with large depth this is because they fail to consider size effect. The prediction of Japanese code and the Eurocode is good for slabs with large amount of flexural reinforcement. They also try to address size effect in a similar way which is good but still unconservative. As large size structures are common in practice specially in foundation structures it is not wise to rely on codes for design. Until sufficient knowledge is acquired it is better to follow conservative approaches. This is because all the codes result in unconservative capacity prediction for large size structures that are lightly reinforced.

Based on the parametric study performed a simple empirical equation is proposed. The coefficient of variation and the R^2 value of the proposed equation are of 0.142 and 97.6% respectively which is better than all the codes except the Japanese code. With regards to R^2 value the Japanese code gives the better prediction which is 98.4%.

References

[1] Nasim S. et al., *Investigation of punching shear behavior of flat slabs with different types and arrangements of shear reinforcement*, **Case Studies in Construction Materials, 16,** 2022, p. e01028. DOI: 10.1016/j.cscm.2022.e01028.

[2] Valença, Jónatas, and Ricardo N. F. Carmo. *Evaluation of the Shear Transfer Mechanisms in Reinforced Concrete Beams Using Photogrammetry*, **Structural Concrete V21 no. 1,** April 5, 2019, pp333–48., DOI.org/10.1002/suco.201800279.

[3] Graf. O., *Experiments on the resistance of reinforced concrete slabs under concentrated load near one support*, **German Committee for Reinforced Concrete**, **Issue 73**, 1933, pp. 10-16.

[4] Moe. J, *Shearing Strength of Reinforced Concrete Slabs and Footings under Concentrated Loads,* **Technical report‖, Portland Cement Association-Research and Development Laboratories,** 1961, p. 72.

[5] Maryouk. H., Hussein. A., *Experimental Investigation on the Behavior of High-Strength Concrete Slabs,* **ACI Structural Journal**, **V. 88 No. 6,** Nov.-Dec. 1991, pp. 701-713., DOI.org/10.14359/1261.

[6] Hallgren. M., *Punching Shear Capacity of Reinforced High Strength Concrete Slabs*, **PhD-Thesis, KTH Stockholm, TRITA-BKN. Bulletin No. 23**, 1996, 150p.

[7] Zsutty. T.C., *Beam Shear Strength Prediction by analysis of Existing data*, **Proceeding of** ACI. V.65, Nov. 1968, pp.943., DOI.org/10.14359/7526.

[8] Talbot. A. N., *Reinforced Concrete Wall and Column Footings*, **ACI Journal Proceedings Vol 45, no. 10**, 1948, DOI.org/10.14359/12107.

[9] Elstner, R. C., Hognestad, E., *Shearing Strength of Reinforced Concrete Slabs,* **ACI Structural Journal**, **V.53, No.1**, Jul. 1956, pp.29-58, DOI.org/10.14359/11501.

[10] Marzouk, H.M. and Hussein, A. *Punching Shear Analysis of Reinforced High- Strength Concrete Slabs,* **Canadian Journal of Civil Engineering, V.18 No.6**, 1991, pp.954- 963, DOI.org/10.1139/l91-118.

[11] Saaeed, B. G., *Strength of Reinforced Concrete Slabs for Punching Shear Stress*, **MSc. thesis, University of** Salahaddin-Hawler. Jul.1989.

[12] Gardner, N. J., Shao, X., *Punching Shear of Continuous Flat Reinforced Concrete Slabs*, **ACI Structural Journal, V. 93 No. 2**, Mar.-Apr.1996, pp 218-228, DOi.org/10.14359/1494.

[13] Ghannoum, C. M., *Effect of High-Strength Concrete on the Performance of Slab-Column Specimens*, **MSc. thesis, McGill University, Canada**. Nov. 1998.

[14] Stein, T., Ghali, A. and Dilger, W., *Distinction between Punching and Flexural Failure Modes of Flat Plates*, **ACI Structural Journal**. **V.104 No. 4,** May/Jun. 2007, DOI.org/10.14359/18626.

[15] Kuchma, D & Collins, M.P. *Advances in understanding shear performance of concrete structures,* **Progress in structural engineering and material, Vol I4,** 1998. PP360-369, DOI.org/10.1002/pse.2260010404

[16] Bazant, Z. P., & Kim, J. K. *Size effect in shear failure of longitudinally reinforced beams,* **Journal of the American Concrete Institute**, **V 81 no 5,** 1984, pp456-468., DOI.org/10.14359/10696.

[17] Bazant, Z. P. and Cao, Z., *Size Effect in Punching Shear Failure of Slabs,* **ACI Structural Journal**, **V 84 No 1,** Feb.1987, pp 44-53. DOI.org/10.14359/2785

[18] Lim, F. K. and Rangan, B.V., *Studies on Concrete Slabs with Stud Shear Reinforcement in Vicinity of Edge and Corner Columns,* **ACI Structural Journal, Vol.92, No.5**, Sep.-Oct. 1995, pp.515-525. DOI.org/10.14359/902.

[19] Guandalini, S., Burdet, O.L. & Muttoni, A., *Punching Tests of Slabs with Low Reinforcement Ratios,* **ACI Structural Journal, 106(1),** 2009, pp87-95. DOI.org/10.14359/56287.

[20] Fernández Ruiz M., Mirzaei Y., Muttoni A., *Post-Punching Behavior of Flat Slabs,* **ACI Structural Journal, V. 110, no 5**, USA, 2013, pp. 801-812. DOI.org/10.14359/51685833.

[21] Ozbolt J, Li YJ, Kozar I. *Microplane model for concrete with relaxed kinematic constraint*. **Int J Solids Struct Vol38, no. 16**, April 2001, pp2683–2711, DOI.org/10.1016/s0020-7683(00)00177-3.

[22] LONG, A. E.,A *Two-Phase Approach to the Prediction of Punching Strength of Slabs*, **Journal of the American Concrete Institute, Proceedings, V. 72, No. 2,** Feb. 1975, pp. 37-45. DOI.org/10.14359/11113.

[23] REGAN, P. E., *Behavior of reinforced concrete flat slabs,* **Construction Industry Research and Information Association**, **London**, **Report 89,** Feb. 1981, p 89.

[24] Muttoni, A., and Schwartz, J., *Behavior of Beams and Punching in Slabs without Shear Reinforcement*, **IABSE Colloquium, V. 62, Zurich, Switzerland**, 1991, pp. 703-708. DOI.org/10.1680/jmacr.16.00099.

[25] Li KKL. *The influence of size on punching shear strength of concrete slabs* **MEng Thesis Department of civil engineering and applied mechanics Montreal, Quebec: McGill University,** 2000. p. 78.

[26] Eurocode 2 - *Design of Concrete Structures – Part 1-1— General Rules and Rules for Buildings*," **EN 1992-1-1, Brussel**s, Belgium, 2004, 225 pp.

[27] ACI Committee 318, *Building Code Requirements for Structural Concrete* (**ACI 318-08) and Commentary, American Concrete Institute**, Farmington Hills, MI, 2005, 465 pp.

[28] CSA Standard A23.3-94 (1994), *Design of Concrete Structures,* **Canadian Portland Cement Association, Rexdale, Ontario, Canada**, 1994.

[29] JSCE guideline for concrete, *Standard Specification for concrete structures, No 15, 2007*

[30] *Base GD. Some tests on the punching shear strength of reinforced concrete slabs*. **Cement and Concrete Association, Slough, Technical Report, TRA/321,** 1959. pp

[31] Taylor R, Hayes B. *Some tests on the effect of edge restraint on punching shear in reinforced concrete slabs.* **Magazine of Concrete Research, Vol 17 No 50,** March 1965, pp39–44. DOI.org/10.1680/macr.1965.17.50.39.

[32] Criswell ME., *Static and dynamic response of reinforced concrete slab-column connections, Shear in reinforced concrete.* **ACI Structral Journal, Detroit, SP 42, Vol. 2, Part 4,** 1974. p. 721–46.

[33] Regan PE., *Design of reinforced concrete slabs.* **Construction industry research and information association project record V220**, London; 1978.

[34] Regan PE., *Symmetric punching of reinforced concrete slabs*, **Magazine of Concrete Research, Vol 36 No 136**, 1986, pp. 115–28. DOI.org/10.1680/macr.1986.38.136.115.

[35] Tomaszewicz, A., *Punching Shear Capacity of Reinforced Concrete Slabs.* **SINTEF Structures and Concrete, Trondheim**, *Report No. STF70 A93082,* 1993 pp. 36.

[36] Rankin GIB, Long AE., *Predicting the punching strength of conventional slab-column specimens,* **ICE proceedings -structures and buildings, No. 82,** April 1987, p. 327–46. DOI.org/10.1680/iicep.1987.382.

[37] Li KKL. *The influence of size on punching shear strength of concrete slabs* **MEng Thesis Department of civil engineering and applied mechanics Montreal, Quebec: McGill University,** 2000. p. 78.

[38] Salim W, Sebastian WM., *Punching shear failure in reinforced concrete slabs with compressive membrane action,* **ACI Structral Journal, Vol 100, no. 4**, 2003 DOI.org/10.14359/12656.

[39] Chen CC, Li CY., *Punching shear strength of reinforced concrete slabs strengthened with glass fiber-reinforced polymer laminates,* **ACI Structural Journal 102, no. 4,** 2005, pp 535–42. DOI.org/10.14359/14557.

[40] Rizk E, Marzouk H, Hussein A., *Punching shear of thick plates with and without shear reinforcement*, **ACI Structural Journal 108, no. 5,** 2011, pp. 581–91. DOI.org/ 10.14359/51683215.

[41] Sagaseta J, Muttoni A, Ruiz MF, *Tassinari L., Non-axis-symmetrical punching shear around internal columns of RC slabs without transverse reinforcement,* **Magazine of Concrete Research, Vol 63 No 6,** 2011, pp441–57. DOI.org/10.1680/macr.10.00098.

[42] Einpaul J, Bujnak J, Ruiz MF, Muttoni A. *Study on influence of column size and slab slenderness on punching strength,* **ACI Structural Journal, 113 no 1. ,**January – February 2016, pp135–45. DOI.org/10.14359/51687945.

[43] Kinnunen S, Nylander H., *Punching of concrete slabs without shear reinforcement*. Stockholm, Sweden **Transactions of the Royal Institute of Technology**; 1960. p. 112.

[44] Dragosavic M, Van Den Beukel A., *Punching shear.* **Heron, Delft**, **Vol. 20, No. 2;** 1974, pp. 48.

[45] Collins, M.P. & Kuchma, D. *How safe are our large, lightly reinforced concrete beams, slabs, and footings?* **ACI Structural Journal Vol 96 No 4,** 1999, pp. 482-490. DOI.org/10.14359/684.

[46] Yoneda, T., T. Ishida, K. Maekawa, E. Gebreyouhannes, and T. Mishima., *Simulation of early-age cracking due to drying shrinkage based on a multi-scale constitutive model,* **Poromechanics** V, June 18, 2013, DOI.org/10.1061/9780784412992.069.

[47] Akanshu S, G.R. Reddy, R. Eligehausens, K.K. Vaze , *Modelling Beam-column joints in performance analysisof Reinforced Concrete Frame Structure,* **Structural Engineering Convention Conference: SEC,** 2012.

[48] Akanshu S, G. Genesio, G. R. Reddy and R. Eligehausen, *Nonlinear dynamic analysis using microplane model for concrete and bond slip model for prediction of behavior of nonseismically detailed RCC beam-column joints,* **Journal of structural engineering, Vol 36 No 4,** 2009, pp. 250-257.

[49] Joško O., Akanshu S, *Numerical simulation of reinforced concrete beams with different shear reinforcements under dynamic impact loads,* **International Journal of Impact Engineering Vol 38 No 12**, 2011, pp940-950. DOI.org/10.1016/ j.ijimpeng.2011.08.003.

[50] M Tonidis, J Bošnjak, A Sharma, *Post-fire performance of RC beams with critical lap splices–Numerical parametric study,* **Journal of Building Engineering, 44,** 2021, DOI.org/10.1016/j.jobe.2021.102637.

[51] Eligehausen et al., *Behavior and design of adhesive bonded anchor,* **ACI Structural Journal Vol 103 No 6**, 2006, pp. 822-831. DOI.org/10.14359/18234.

Appendix

Table 5 Comparison of Punching shear prediction capacity of ACI, Canadian Eurocode Japanese code and Proposed equation with experimental results from literature

Slab Name	f_c' (MPa)	ρ	d (mm)	C (mm)	V_{exp} (kN)	V_{ACI} (kN)	V_{EC} (kN)	V_{Jap} (kN)	V_{Can} (kN)	V_{pro}	$V_{EXP}/V_{ACI\,Str}$	V_{EXP}/V_{EC}	V_{EXP}/V_{Jap}	V_{EXP}/V_{Can}	V_{ex}/V_{pro} AVG1
Calibration With ρ =0.49% [V_Prop1]														
PM2C25	20	0.49%	97.4	130	161.7	132.1	130.9	121.5	150.6	164.9	1.22	1.24	1.33	1.07	0.98
PM2C35	28	0.49%	97.4	130	192.8	156.3	146.4	143.8	178.1	188.6	1.23	1.32	1.34	1.08	1.02
PM2C45	36.5	0.49%	97.4	130	223.4	178.4	159.9	164.2	203.4	209.7	1.25	1.40	1.36	1.10	1.07
PM2C55	44	0.49%	97.4	130	229.9	195.9	170.2	180.3	223.3	226.0	1.17	1.35	1.28	1.03	1.02
PM2C65	52	0.49%	97.4	130	234.4	213.0	179.9	196.0	242.8	241.6	1.10	1.30	1.20	0.97	0.97
PM2C100	80	0.49%	97.4	130	250.8	264.1	207.7	243.1	301.1	287.0	0.95	1.21	1.03	0.83	0.87
PM2ρ0.49	36.5	0.49%	97.4	130	223.4	178.4	159.9	164.2	203.4	209.7	1.25	1.40	1.36	1.10	1.07
PM2ρ0.82	36.5	0.82%	97.4	130	230.6	178.4	189.9	194.9	203.4	244.7	1.29	1.21	1.18	1.13	0.94
PM2ρ1.0	36.5	1.00%	97.4	130	261.0	178.4	202.8	208.3	203.4	259.7	1.46	1.29	1.25	1.28	1.00
PM2ρ1.5	36.5	1.50%	97.4	130	297.4	178.4	232.2	238.4	203.4	293.3	1.67	1.28	1.25	1.46	1.01
PM2ρ2.0	36.5	2.00%	97.4	130	297.4	178.4	255.6	262.4	203.4	319.8	1.67	1.16	1.13	1.46	0.93
PM2D100	36.5	0.49%	73.5	130	115.52	120.4	99.8	107.3	137.3	139.3	0.96	1.16	1.08	0.84	0.83
PM2D125	36.5	0.49%	97.4	130	188.8	178.4	159.9	164.2	203.4	209.7	1.06	1.18	1.15	0.93	0.90
PM2D150	36.5	0.49%	121.5	130	275.97	246.1	234.0	232.1	280.5	288.9	1.12	1.18	1.19	0.98	0.96
PM2D175	36.5	0.49%	145.6	130	345.4	323.3	322.2	310.9	368.6	375.8	1.07	1.07	1.11	0.94	0.92
PM2D200	36.5	0.49%	169.9	130	430	410.3	424.5	400.6	467.7	469.7	1.05	1.01	1.07	0.92	0.92
PM2D225	36.5	0.49%	194.1	130	572.2	506.9	540.9	501.2	577.9	570.1	1.13	1.06	1.14	0.99	1.00
PM2D250	36.5	0.49%	218.5	130	667.3	613.2	657.1	597.4	699.1	676.5	1.09	1.02	1.12	0.95	0.99
PM2D500	36.5	0.49%	463.1	130	2068.8	2212.5	2290.1	1880.7	2522.2	2011.0	0.94	0.90	1.10	0.82	1.03
PM2P10	36.5	0.49%	97.4	100	171.4	154.9	148.9	146.7	176.6	196.4	1.11	1.15	1.17	0.97	0.87
PM2P13	36.5	0.49%	97.4	130	188.8	178.4	159.9	164.2	203.4	209.7	1.06	1.18	1.15	0.93	0.90
PM2P16	36.5	0.49%	97.4	160	193.3	202.0	170.9	181.5	230.2	220.9	0.96	1.13	1.06	0.84	0.88
PM2P20	36.5	0.49%	97.4	200	208.5	233.3	185.6	204.3	266.0	233.5	0.89	1.12	1.02	0.78	0.89
PM2P25	36.5	0.49%	97.4	250	215.0	272.6	203.9	232.7	310.7	246.9	0.79	1.05	0.92	0.69	0.87
PM2P30	36.5	0.49%	97.4	300	228.5	311.8	222.3	261.0	355.4	258.5	0.73	1.03	0.88	0.64	0.88
Calibration With ρ =1.5% [V_Prop2]														
PMρC25	28	1.50%	92.1	130	237.7	144.3	193.3	191.6	164.5	243.3	1.65	1.23	1.24	1.44	0.98
PMρC35	36	1.50%	92.1	130	293.7	163.6	210.2	217.3	186.6	269.0	1.79	1.40	1.35	1.57	1.09
PMρC45	44	1.50%	92.1	130	298.7	180.9	224.8	240.2	206.2	291.5	1.65	1.33	1.24	1.45	1.02
PMρC55	52	1.50%	92.1	130	315.6	196.7	237.6	261.1	224.2	311.6	1.60	1.33	1.21	1.41	1.01
PMρC65	60	1.50%	92.1	130	337.9	211.3	249.2	280.5	240.8	330.0	1.60	1.36	1.20	1.40	1.02
PMρC75	68	1.50%	92.1	130	357.7	224.9	259.8	298.6	256.4	346.9	1.59	1.38	1.20	1.39	1.03
PMρC85	76	1.50%	92.1	130	383.6	237.8	269.7	315.7	271.1	362.7	1.61	1.42	1.22	1.42	1.06
PMρC100	88	1.50%	92.1	130	390.0	255.9	283.2	339.7	291.7	384.6	1.52	1.38	1.15	1.34	1.01
PMρC120	104	1.50%	92.1	130	416.3	278.1	299.4	369.3	317.1	411.2	1.50	1.39	1.13	1.31	1.01
PMρρ0.49	36	0.49%	92.1	130	223.4	163.6	144.8	149.6	186.6	192.3	1.37	1.54	1.49	1.20	1.16
PMρρ0.80	36	0.80%	92.1	130	230.6	163.6	170.5	176.2	186.6	222.8	1.41	1.35	1.31	1.24	1.04
PMρρ1.0	36	1.00%	92.1	130	261.0	163.6	183.6	189.8	186.6	238.2	1.60	1.42	1.38	1.40	1.10
PMρρ1.5	36	1.50%	92.1	130	297.4	163.6	210.2	217.3	186.6	269.0	1.82	1.41	1.37	1.59	1.11
PMρρ2.0	36	2.00%	92.1	130	297.4	163.6	231.4	239.1	186.6	293.2	1.82	1.29	1.24	1.59	1.01
PMρρ2.5	36	2.50%	92.1	130	302.1	163.6	231.4	257.6	186.6	313.5	1.85	1.31	1.17	1.62	0.96
PMρD100	36	1.50%	68.9	130	155.3	109.7	130.1	140.9	125.1	176.8	1.41	1.19	1.10	1.24	0.88
PMρD125	36	1.50%	92.1	130	241.8	163.6	210.2	217.3	186.6	269.0	1.48	1.15	1.11	1.30	0.90
PMρD150	36	1.50%	115.5	130	397.7	226.8	309.7	308.8	258.5	373.4	1.75	1.28	1.29	1.54	1.07
PMρD175	36	1.50%	139.0	130	521.2	299.1	428.7	415.6	341.0	488.6	1.74	1.22	1.25	1.53	1.07
PMρD200	36	1.50%	162.6	130	624.5	380.8	567.4	537.5	434.1	613.6	1.64	1.10	1.16	1.44	1.02
PMρD225	36	1.50%	186.4	130	798.0	471.8	725.9	674.7	537.8	747.6	1.69	1.10	1.18	1.48	1.07

PMρD250	36	1.50%	210.2	130	952.7	572.1	893.2	814.4	652.2	890.0	1.67	1.07	1.17	1.46	1.07
PMρD300	36	1.50%	257.8	130	1223.5	799.8	1240.3	1100.4	911.8	1196.6	1.53	0.99	1.11	1.34	1.02
PMρD400	36	1.50%	354.0	130	1656.7	1370.7	2096.1	1781.5	1562.6	1895.0	1.21	0.79	0.93	1.06	0.87
PMρD500	36	1.50%	450.7	130	2620.7	2093.5	3158.8	2597.7	2386.5	2689.3	1.25	0.83	1.01	1.10	0.97
PMρD500	36	0.49%	463.1	130	2068.0	2197.3	2279.6	1867.8	2504.9	1999.9	0.94	0.91	1.11	0.83	1.03
PMρP10	36	1.50%	92.1	100	251.8	141.5	195.2	193.5	161.4	251.9	1.78	1.29	1.30	1.56	1.00
PMρP13	36	1.50%	92.1	130	293.7	163.6	210.2	217.3	186.6	269.0	1.79	1.40	1.35	1.57	1.09
PMρP16	36	1.50%	92.1	160	314.2	185.7	225.2	240.8	211.8	283.3	1.69	1.39	1.30	1.48	1.11
PMρP20	36	1.50%	92.1	200	363.9	215.2	245.3	271.9	245.3	299.6	1.69	1.48	1.34	1.48	1.21
PMρP25	36	1.50%	92.1	250	372.8	252.1	270.4	310.6	287.3	316.8	1.48	1.38	1.20	1.30	1.18
PMρP30	36	1.50%	92.1	300	414.2	288.9	295.4	349.0	329.3	331.5	1.43	1.40	1.19	1.26	1.25
Marzouk and Hussien [1991] [5]															
NS1	42	1.47%	95	150	320	201.1	242.5	261.8	229.3	308.3	1.59	1.32	1.22	1.40	1.04
HS1	67	0.50%	95	150	178	254.0	197.1	230.1	289.6	268.1	0.70	0.90	0.77	0.61	0.66
HS2	70	0.84%	95	150	249	259.6	238.7	280.7	296.0	319.9	0.96	1.04	0.89	0.84	0.78
HS7	74	1.19%	95	150	356	267.0	273.2	324.2	304.3	363.2	1.33	1.30	1.10	1.17	0.98
HS3	69	1.47%	95	150	356	257.8	286.3	335.8	293.9	376.2	1.38	1.24	1.06	1.21	0.95
HS4	66	2.37%	90	150	418	234.0	285.6	355.0	266.7	394.1	1.79	1.46	1.18	1.57	1.06
NS2	30	0.94%	120	150	396	236.6	277.6	273.0	269.7	331.1	1.67	1.43	1.45	1.47	1.20
HS5	68	0.64%	95	150	365	255.9	215.8	252.5	291.7	291.3	1.43	1.69	1.45	1.25	1.25
HS6	70	0.94%	120	150	489	361.4	368.2	417.0	412.0	464.6	1.35	1.33	1.17	1.19	1.05
HS8	69	1.11%	120	150	436	358.8	386.8	437.1	409.1	485.1	1.22	1.13	1.00	1.07	0.90
HS9	74	1.61%	120	150	543	371.6	448.2	512.3	423.6	557.7	1.46	1.21	1.06	1.28	0.97
HS10	80	2.33%	120	150	645	386.4	494.4	602.7	440.5	642.9	1.67	1.30	1.07	1.46	1.00
HS11	70	0.95%	70	150	196	171.8	151.2	186.8	195.8	213.2	1.14	1.30	1.05	1.00	0.92
HS12	75	1.52%	70	150	258	177.8	181.0	226.2	202.7	252.4	1.45	1.43	1.14	1.27	1.02
HS13	68	2.00%	70	150	267	169.3	191.8	235.8	193.0	263.3	1.58	1.39	1.13	1.38	1.01
HS14	72	1.47%	95	220	498	338.6	335.7	422.0	386.0	421.1	1.47	1.48	1.18	1.29	1.18
HS15	71	1.47%	95	300	560	421.6	385.7	507.9	480.6	452.6	1.33	1.45	1.10	1.17	1.24
Elstner and Hognestad [1956] [9]															
A-1a	14.1	1.15%	117.6	254	303	218.8	267.2	253.1	249.4	287.7	1.38	1.13	1.20	1.21	1.05
A-1b	25.3	1.20%	117.6	254	366	293.1	329.4	343.9	334.1	368.2	1.25	1.11	1.06	1.10	0.99
A-1c	29.1	1.20%	117.6	254	357	314.3	345.1	368.9	358.3	389.3	1.14	1.03	0.97	1.00	0.92
A-1d	36.9	1.20%	117.6	254	352	353.9	373.5	415.4	403.5	428.1	0.99	0.94	0.85	0.87	0.82
A-1e	20.3	1.20%	117.6	254	357	262.5	306.1	308.1	299.3	337.1	1.36	1.17	1.16	1.19	1.06
A-2a	13.7	2.47%	114.3	254	334	207.8	304.2	309.1	236.8	343.2	1.61	1.10	1.08	1.41	0.97
A-2b	19.6	2.50%	114.3	254	401	248.5	342.8	371.2	283.3	397.5	1.61	1.17	1.08	1.42	1.01
A-2c	37.5	2.50%	114.3	254	468	343.7	425.5	513.5	391.8	515.3	1.36	1.10	0.91	1.19	0.91
A-7b	28	2.50%	114.3	254	513	297.0	386.1	443.7	338.6	458.5	1.73	1.33	1.16	1.52	1.12
A-3a	12.8	3.70%	114.3	254	357	200.8	297.4	331.6	228.9	377.1	1.78	1.20	1.08	1.56	0.95
A-3b	22.7	3.70%	114.3	254	446	267.4	360.0	441.6	304.9	474.2	1.67	1.24	1.01	1.46	0.94
A-3c	26.6	3.70%	114.3	254	535	289.5	379.5	478.0	330.0	505.3	1.85	1.41	1.12	1.62	1.06
A-3d	34.6	3.70%	114.3	254	549	330.2	414.3	545.1	376.4	561.3	1.66	1.33	1.01	1.46	0.98
A-4	26.2	1.20%	117.6	356	401	380.1	387.7	429.6	433.3	406.2	1.05	1.03	0.93	0.93	0.99
A-5	27.8	2.50%	114.3	356	535	377.9	449.2	543.9	430.8	497.5	1.42	1.19	0.98	1.24	1.08
A-6	25.1	3.70%	114.3	356	499	359.1	434.2	571.2	409.4	537.1	1.39	1.15	0.87	1.22	0.93
A-13	26.3	0.55%	120.6	356	236	393.0	311.0	343.4	448.0	333.9	0.60	0.76	0.69	0.53	0.71
B-1	14.2	0.50%	114.3	254	179	211.5	193.9	184.8	241.1	215.6	0.85	0.92	0.97	0.74	0.83
B-2	47.7	0.50%	114.3	254	201	387.7	290.5	338.7	441.9	350.1	0.52	0.69	0.59	0.45	0.57
B-4	47.8	0.99%	114.3	254	334	388.1	365.0	425.7	442.4	430.1	0.86	0.92	0.78	0.75	0.78
B-9	44	2.00%	114.3	254	506	372.3	448.8	516.4	424.4	513.8	1.36	1.13	0.98	1.19	0.98
B-11	13.5	3.00%	114.3	254	330	206.2	302.7	327.4	235.1	361.7	1.60	1.09	1.01	1.40	0.91
B-14	50.5	3.00%	114.3	254	580	398.9	469.9	633.2	454.7	613.1	1.45	1.23	0.92	1.28	0.95
Base [1959] [30]															
A	26.5	1.08%	57.3	102	93.9	62.7	71.24	72.66	71.42	102.07	1.50	1.32	1.29	1.31	0.92
B	28.6	1.08%	57.3	102	103.9	65.1	73.08	75.48	74.20	105.23	1.60	1.42	1.38	1.40	0.99

C	26.2	1.08%	57.3	102	97.9	62.3	70.97	72.24	71.02	101.60	1.57	1.38	1.36	1.38	0.96
D	27.4	1.08%	57.3	102	103.9	63.7	72.04	73.88	72.63	103.44	1.63	1.44	1.41	1.43	1.00
E	29.8	0.73%	57.3	102	81.9	66.4	64.81	67.40	75.74	94.84	1.23	1.26	1.22	1.08	0.86
F	27.8	0.73%	57.3	102	81.9	64.2	63.33	65.10	73.15	92.24	1.28	1.29	1.26	1.12	0.89
G	29.1	1.64%	57.3	102	112.9	65.7	84.32	87.34	74.84	119.90	1.72	1.34	1.29	1.51	0.94
H	26.4	1.64%	57.3	102	99.9	62.5	81.63	83.19	71.29	115.32	1.60	1.22	1.20	1.40	0.87
J	28.1	3.27%	57.3	102	117.9	64.5	89.13	108.14	73.55	145.56	1.83	1.32	1.09	1.60	0.81

Moe [1961] [4]

S1-60	23.3	1.06%	114.3	254	389	270.9	293.9	304.1	308.9	329.3	1.44	1.32	1.28	1.26	1.18
S5-60	22.2	1.06%	114.3	203	393	227.8	265.1	262.4	259.7	305.4	1.72	1.48	1.50	1.51	1.29
S7-70	24.5	1.06%	114.3	254	343	277.8	298.8	311.8	316.7	336.0	1.23	1.15	1.10	1.08	1.02
S5-70	23.1	1.06%	114.3	203	378	232.4	268.6	267.7	265.0	310.3	1.63	1.41	1.41	1.43	1.22
H1	26.1	1.15%	114.3	254	372	286.8	313.6	330.7	326.9	353.2	1.30	1.19	1.12	1.14	1.05
R2	26.6	1.15%	114.3	152	372	209.3	263.1	256.1	238.6	313.0	1.78	1.41	1.45	1.56	1.19
M1A	20.9	1.50%	114.3	305	433	292.1	344.6	360.6	333.0	366.3	1.48	1.26	1.20	1.30	1.18

Taylor & Hayes [1965] [31]

2S2	26	1.57%	63.5	51	72.4	49.4	78.9	70.8	56.4	110.5	1.46	0.92	1.02	1.28	0.66
2S3	24.6	1.57%	63.5	76	92.9	58.6	85.2	80.5	66.8	119.4	1.59	1.09	1.15	1.39	0.78
2S4	23.2	1.57%	63.5	102	87.4	67.5	91.4	89.6	76.9	125.6	1.29	0.96	0.97	1.14	0.70
2S5	22.1	1.57%	63.5	127	98.4	75.8	97.4	98.2	86.4	130.1	1.30	1.01	1.00	1.14	0.76
2S6	18.4	1.57%	63.5	152	98.4	78.3	98.6	99.3	89.2	126.4	1.26	1.00	0.99	1.10	0.78
3S2	22.8	3.14%	63.5	51	79.9	46.3	81.8	83.6	52.8	129.1	1.73	0.98	0.96	1.51	0.62
3S4	22.6	3.14%	63.5	102	117.4	66.6	98.2	111.5	75.9	153.0	1.76	1.20	1.05	1.55	0.77
3S6	21.7	1.57%	63.5	152	152.8	85.0	104.2	107.8	96.9	135.1	1.80	1.47	1.42	1.58	1.13

Criswell [1974] [32]

S2075-1	32.5	0.75%	120.6	254	291	343.4	318.7	345.6	391.5	366.6	0.85	0.91	0.84	0.74	0.79
S2075-2	29.1	0.75%	122.2	254	273	330.7	313.7	333.2	376.9	357.5	0.83	0.87	0.82	0.72	0.76
S2150-1	29.7	1.50%	124	254	464	340.6	407.4	433.2	388.3	453.2	1.36	1.14	1.07	1.20	1.02
S2150-2	30.2	1.50%	122.2	254	441	336.8	400.1	427.7	384.0	446.7	1.31	1.10	1.03	1.15	0.99
S4075-1	26.7	0.75%	127	508	343	555.6	450.4	521.8	633.4	434.3	0.62	0.76	0.66	0.54	0.79
S4075-2	32.3	0.75%	124	508	330	593.9	463.7	556.4	677.0	452.7	0.56	0.71	0.59	0.49	0.73
S4150-1	35.5	1.50%	125.5	508	581	631.6	613.5	746.5	720.0	589.0	0.92	0.95	0.78	0.81	0.99
S4150-2	35.8	1.50%	125.5	508	582	634.3	615.2	749.6	723.1	591.0	0.92	0.95	0.78	0.80	0.98

Regan [1978,1986] [33][34]

I/2	23.4	1.20%	77	200	176	137.6	148.9	158.1	156.8	181.9	1.28	1.18	1.11	1.12	0.97
I/4	32.3	0.92%	77	200	194	161.6	151.8	170.0	184.3	191.1	1.20	1.28	1.14	1.05	1.02
I/6	21.9	0.75%	79	200	165	137.5	129.6	135.5	156.8	159.7	1.20	1.27	1.22	1.05	1.03
I/7	30.4	0.80%	79	200	186	162.0	147.7	163.2	184.7	185.6	1.15	1.26	1.14	1.01	1.00
II/1	25.76	1.20%	77	200	194	144.3	153.8	165.9	164.5	189.0	1.34	1.26	1.17	1.18	1.03
II/2	23.44	1.20%	77	200	176	137.7	149.0	158.2	157.0	182.0	1.28	1.18	1.11	1.12	0.97
II/3	27.44	0.92%	77	200	194	149.0	143.7	156.7	169.8	179.0	1.30	1.35	1.24	1.14	1.08
II/4	32.32	0.92%	77	200	194	161.7	151.8	170.1	184.3	191.1	1.20	1.28	1.14	1.05	1.02
II/5	28.16	0.75%	79	200	165	156.0	140.9	153.7	177.8	176.6	1.06	1.17	1.07	0.93	0.93
II/6	21.92	0.75%	79	200	165	137.6	129.6	135.6	156.9	159.7	1.20	1.27	1.22	1.05	1.03
II/7	30.4	0.80%	79	200	186	162.0	147.7	163.2	184.7	185.6	1.15	1.26	1.14	1.01	1.00
V/4	36.24	0.80%	118	102	285	208.4	246.8	236.7	237.5	301.1	1.37	1.15	1.20	1.20	0.95

Tomaszewicz [1993] [35]

65-1-1	64.3	1.50%	275	200	2050	1396.6	1790.0	1831.6	1592.1	1845.5	1.47	1.15	1.12	1.29	1.11
65-2-1	70.2	1.70%	200	150	1200	782.0	1103.6	1154.5	891.5	1163.9	1.53	1.09	1.04	1.35	1.03
95-1-1	83.7	1.50%	275	200	2250	1593.4	1954.4	2089.7	1816.5	2050.8	1.41	1.15	1.08	1.24	1.10
95-1-3	89.9	2.50%	275	200	2400	1651.4	2203.0	2567.8	1882.6	2459.8	1.45	1.09	0.93	1.27	0.98
95-2-1	88.2	1.70%	200	150	1100	876.5	1190.8	1294.1	999.3	1275.2	1.25	0.92	0.85	1.10	0.86
95-2-1D	86.7	1.70%	200	150	1300	869.1	1184.1	1283.0	990.7	1266.4	1.50	1.10	1.01	1.31	1.03
95-2-3	89.5	2.60%	200	150	1450	883.0	1263.3	1501.9	1006.6	1457.0	1.64	1.15	0.97	1.44	1.00
95-2-3D	80.3	2.60%	200	150	1250	836.4	1218.4	1422.6	953.5	1395.1	1.49	1.03	0.88	1.31	0.90
95-2-3D+	98	2.60%	200	150	1450	924.0	1302.1	1571.6	1053.3	1510.9	1.57	1.11	0.92	1.38	0.96

95-3-1	85.1	1.80%	88	100	330	203.5	255.2	294.2	232.0	351.4	1.62	1.29	1.12	1.42	0.94
115-1-1	112	1.50%	275	200	2450	1843.2	2153.7	2417.4	2101.3	2304.2	1.33	1.14	1.01	1.17	1.06
115-2-1	119	1.70%	200	150	1400	1018.1	1315.9	1503.1	1160.7	1437.5	1.38	1.06	0.93	1.21	0.97
115-2-3	108	2.60%	200	150	1550	969.9	1344.9	1649.9	1105.7	1570.7	1.60	1.15	0.94	1.40	0.99

Rankin & Long [1987] [36]

1	30.72	0.42%	40.5	100	36.42	42.1	31.2	34.3	47.9	49.1	0.87	1.17	1.06	0.76	0.74
2	30.72	0.56%	40.5	100	49.08	42.1	34.2	37.7	47.9	53.4	1.17	1.44	1.30	1.02	0.92
3	30.72	0.69%	40.5	100	56.55	42.1	36.7	40.4	47.9	56.9	1.34	1.54	1.40	1.18	0.99
4	34.8	0.82%	40.5	100	56.18	44.8	40.5	45.6	51.0	63.0	1.26	1.39	1.23	1.10	0.89
5	34.8	0.88%	40.5	100	57.27	44.8	41.5	46.7	51.0	64.4	1.28	1.38	1.23	1.12	0.89
6	34.8	1.03%	40.5	100	56.58	44.8	43.6	49.1	51.0	67.4	1.26	1.30	1.15	1.11	0.84
7	29.68	1.16%	40.5	100	70.94	41.3	43.1	47.3	47.1	65.6	1.72	1.64	1.50	1.51	1.08
8	29.68	1.29%	40.5	100	71.09	41.3	44.7	49.0	47.1	67.7	1.72	1.59	1.45	1.51	1.05
9	29.68	1.45%	40.5	100	78.6	41.3	46.5	50.9	47.1	70.2	1.90	1.69	1.54	1.67	1.12
10	29.2	0.52%	40.5	100	43.59	41.0	32.8	35.8	46.7	51.1	1.06	1.33	1.22	0.93	0.85
11	29.2	0.80%	40.5	100	55	41.0	37.9	41.4	46.7	58.3	1.34	1.45	1.33	1.18	0.94
12	29.2	1.11%	40.5	100	67.06	41.0	42.2	46.1	46.7	64.3	1.64	1.59	1.45	1.43	1.04
13	34	0.60%	40.5	100	49.39	44.2	36.2	40.6	50.4	56.9	1.12	1.36	1.22	0.98	0.87
14	34	0.69%	40.5	100	52.45	44.2	38.0	42.5	50.4	59.3	1.19	1.38	1.23	1.04	0.88
15	34	1.99%	40.5	100	84.84	44.2	54.0	60.6	50.4	81.5	1.92	1.57	1.40	1.68	1.04
1A	28.8	0.42%	46.5	100	45.19	48.7	37.9	40.4	55.6	58.5	0.93	1.19	1.12	0.81	0.77
2A	28.8	0.69%	46.5	100	66.24	48.7	44.7	47.6	55.6	67.8	1.36	1.48	1.39	1.19	0.98
3A	28.8	1.29%	46.5	100	89.72	48.7	55.0	58.7	55.6	81.8	1.84	1.63	1.53	1.61	1.10
4A	30.88	1.99%	46.5	100	97.43	50.5	65.0	70.2	57.5	95.8	1.93	1.50	1.39	1.69	1.02
1B	37.68	0.42%	35	100	28.85	38.7	26.6	31.1	44.1	43.1	0.75	1.08	0.93	0.65	0.67
2B	37.68	0.69%	35	100	37.63	38.7	31.3	36.6	44.1	50.0	0.97	1.20	1.03	0.85	0.75
3B	37.68	1.29%	35	100	56.67	38.7	38.6	45.1	44.1	60.3	1.47	1.47	1.26	1.29	0.94
4B	30.88	1.99%	35	100	72.52	35.0	41.8	47.2	39.9	63.4	2.07	1.74	1.54	1.82	1.14
1C	27.84	0.42%	53.5	100	62.74	57.8	47.0	48.7	65.9	70.7	1.09	1.34	1.29	0.95	0.89
2C	32.4	0.69%	53.5	100	87.86	62.3	58.2	61.8	71.1	87.0	1.41	1.51	1.42	1.24	1.01
3C	32.4	1.29%	53.5	100	124.14	62.3	71.6	76.1	71.1	105.0	1.99	1.73	1.63	1.75	1.18
4C	27.84	1.99%	53.5	100	125.94	57.8	78.8	81.6	65.9	112.6	2.18	1.60	1.54	1.91	1.12

Li [2000] [37]

P100	39.4	0.98%	100	200	330	251.1	250.2	277.9	286.2	308.0	1.31	1.32	1.19	1.15	1.07
P150	39.4	0.90%	150	200	583	439.4	476.3	495.3	500.9	540.5	1.33	1.22	1.18	1.16	1.08
P200	39.4	0.83%	200	200	904	669.5	762.9	755.9	763.3	800.6	1.35	1.19	1.20	1.18	1.13
P300	39.4	0.76%	300	200	1381	1255.4	1392.0	1294.7	1431.1	1403.6	1.10	0.99	1.07	0.96	0.98
P400	39.4	0.76%	400	300	2224	2343.4	2376.5	2224.5	2671.5	2357.4	0.95	0.94	1.00	0.83	0.94
P500	39.4	0.76%	500	300	2681	3347.7	3414.1	3067.1	3816.4	3258.0	0.80	0.79	0.87	0.70	0.82

Salim & Sebastian [2003] [38]

S1	50.4	1.06%	113	150	369.4	281.3	309.5	335.0	320.7	386.6	1.31	1.19	1.10	1.15	0.96
S2	41.6	1.06%	113	150	290.6	255.6	290.3	304.4	291.4	358.0	1.14	1.00	0.95	1.00	0.81
S3	44.8	1.06%	113	150	402.2	265.2	297.6	315.9	302.4	368.8	1.52	1.35	1.27	1.33	1.09
S4	42.4	1.06%	113	150	394.1	258.0	292.2	307.3	294.1	360.8	1.53	1.35	1.28	1.34	1.09

Chen & Li [2005] [39]

SR1C1F0	16.9	0.59%	70.5	150	103.9	85.2	81.2	79.1	97.1	105.7	1.22	1.28	1.31	1.07	0.98
SR1C2F0	34.4	0.59%	70.5	150	123.8	121.6	102.9	112.8	138.6	140.4	1.02	1.20	1.10	0.89	0.88
SR2C1F0	16.9	1.31%	70.5	150	146.1	85.2	105.9	103.1	97.1	134.3	1.71	1.38	1.42	1.50	1.09
SR2C2F0	34.4	1.31%	70.5	150	225.7	121.6	134.2	147.2	138.6	178.4	1.86	1.68	1.53	1.63	1.27

Guandalin and Motino [2009] [19]

PG1	27.6	1.50%	210	260	1023	691.4	950.6	917.6	788.2	950.3	1.48	1.08	1.11	1.30	1.08
PG3	32.4	0.33%	456	520	2153	3377.7	2347.6	2249.8	3850.6	2355.0	0.64	0.92	0.96	0.56	0.91
PG6	34.7	1.50%	96	130	238	170.4	222.8	227.3	194.3	281.5	1.40	1.07	1.05	1.23	0.85
PG7	34.7	1.50%	100	130	238	180.6	238.8	242.1	205.9	298.7	1.32	1.00	0.98	1.16	0.80
PG11	31.5	0.75%	210	260	763	738.6	788.4	778.0	842.0	813.8	1.03	0.97	0.98	0.91	0.94

yaser and Motino [2010] [20]															
PM1	36.5	0.25%	92.1	130	176	164.8	116.2	120.4	187.8	158.0	1.07	1.51	1.46	0.94	1.11
PM2	36.5	0.50%	92.1	130	224	164.8	146.4	151.7	187.8	194.5	1.36	1.53	1.48	1.19	1.15
PM3	37.8	0.82%	92.1	130	324	167.7	174.7	182.0	191.2	228.8	1.93	1.85	1.78	1.69	1.42
PM4	36.8	1.41%	92.1	130	295	165.5	207.4	215.2	188.6	266.4	1.78	1.42	1.37	1.56	1.11
Rizk et al [2011] [40]															
HSS1	76	0.50%	267.5	400	1722	2075.5	1497.6	1759.6	2366.1	1621.3	0.83	1.15	0.98	0.73	1.06
HSS3	65	1.42%	262.5	400	2090	1869.4	1959.1	2250.1	2131.2	2026.9	1.12	1.07	0.93	0.98	1.03
NSS1	40	1.58%	312.5	400	2234	1877.6	2229.1	2287.0	2140.5	2219.2	1.19	1.00	0.98	1.04	1.01
HSS4	60	1.58%	312.5	400	2513	2299.6	2551.6	2801.0	2621.5	2609.9	1.09	0.98	0.90	0.96	0.96
Sagaseta et al [2011] [41]															
PT22	67	0.82%	196	260	989	975.4	939.6	1066.5	1112.0	1022.9	1.01	1.05	0.93	0.89	0.97
PT31	66.3	1.48%	212	260	1433	1086.4	1285.2	1433.5	1238.4	1362.5	1.32	1.12	1.00	1.16	1.05
Einpaul et al [2016] [39]															
PE4	35.1	1.59%	197	260	985	711.2	952.8	970.2	810.7	970.5	1.39	1.03	1.02	1.21	1.01
PV1	31.1	1.50%	210	260	978	733.9	989.2	974.0	836.6	996.8	1.33	0.99	1.00	1.17	0.98
PE3	34.2	1.54%	204	260	961	738.1	987.1	992.1	841.4	1000.7	1.30	0.97	0.97	1.14	0.96
Kinunnem and Nylander [1960] [43]															
IA30a/24	25.9	1.01%	128	300	430	371.74	384.17	408.08	423.79	415.98	1.16	1.12	1.05	1.01	1.03
IA30a/25	24.6	1.04%	124	300	408	347.69	362.81	384.04	396.37	392.60	1.17	1.12	1.06	1.03	1.04
IA15a/5	26.3	0.80%	117	150	255	213.61	240.73	232.53	243.51	288.09	1.19	1.06	1.10	1.05	0.89
IA15a/6	25.7	0.79%	118	150	275	213.76	241.37	231.95	243.68	287.90	1.29	1.14	1.19	1.13	0.96
Dragosavic and van den Beukel [1974] [44]															
1	30.7	1.20%	30	60	32	19.9	22.2	23.6	22.7	38.3	1.60	1.44	1.35	1.41	0.84
2	30.7	1.20%	30	60	33	19.9	22.2	23.6	22.7	38.3	1.65	1.49	1.40	1.45	0.86
3	27.3	1.20%	60	60	78	50.2	68.7	64.2	57.2	99.7	1.56	1.14	1.21	1.36	0.78
4	30.7	1.20%	30	40	26	15.5	19.3	19.2	17.7	34.6	1.68	1.35	1.35	1.47	0.75
5	22	0.50%	30	60	18	16.9	14.8	14.9	19.2	25.7	1.07	1.21	1.21	0.94	0.70
6	22.2	1.20%	30	60	31.2	17.0	19.9	20.1	19.3	33.6	1.84	1.57	1.55	1.61	0.93
7	22.2	1.73%	30	60	28	17.0	22.5	22.7	19.3	37.5	1.65	1.25	1.23	1.45	0.75
15	24.9	0.60%	30	60	21.1	18.0	16.4	16.9	20.5	28.6	1.17	1.29	1.25	1.03	0.74
16	23.6	0.90%	30	60	26	17.5	18.5	18.8	19.9	31.6	1.49	1.41	1.38	1.30	0.82
17	23.6	1.30%	30	60	26	17.5	20.9	21.3	19.9	35.3	1.49	1.25	1.22	1.30	0.74
18	23.6	1.70%	30	60	30	17.5	22.8	23.3	19.9	38.2	1.72	1.32	1.29	1.50	0.78
19	23.6	2.10%	30	60	30	17.5	24.1	25.0	19.9	40.7	1.72	1.25	1.20	1.50	0.74
20	23.6	2.50%	30	60	30	17.5	24.1	26.4	19.9	42.9	1.72	1.25	1.13	1.50	0.70
Einpaul et al [2016] [42]															
PE11	37.5	0.75%	215.0	166	712	668.8	778.2	736.2	762.5	807.1	1.06	0.91	0.97	0.93	0.88
PE9	44.1	0.74%	218.0	330	935	1057.8	996.6	1074.1	1205.9	1039.1	0.88	0.94	0.87	0.78	0.90
PE12	37.6	0.76%	212.0	660	1206	1511.4	1219.8	1437.0	1723.0	1122.3	0.80	0.99	0.84	0.70	1.07
PE6	38.4	1.46%	215.0	83	656	529.4	882.7	769.9	603.5	836.7	1.24	0.74	0.85	1.09	0.78
PE7	42.5	1.47%	213.0	166	871	701.7	1000.7	967.9	799.9	1024.4	1.24	0.87	0.90	1.09	0.85
PE8	42	1.47%	214.0	330	1091	1005.9	1200.5	1287.2	1146.8	1218.8	1.08	0.91	0.85	0.95	0.90
PE5	36.7	1.50%	210.0	660	1476	1475.7	1499.9	1762.4	1682.3	1344.4	1.00	0.98	0.84	0.88	1.10
											1.36	1.22	1.14	1.19	0.97
											0.31	0.21	0.19	0.28	0.13
											0.23	0.17	0.17	0.23	0.14
											0.52	0.69	0.59	0.45	0.57
											0.900	0.972	0.984	0.900	0.987